SEISMIC SAFETY OF BUILDINGS

Sponsored by National Science Foundation
Grant ENV 76-19021

INTERNAL STUDY REPORT NO. 15

COVARIANCE ANALYSIS OF THE RESPONSE OF BUILDINGS TO EARTHQUAKE LOADING

by

RICARDO BINDER

Supervised by
Professor J. M. Biggs
Professor E. H. Vanmarcke

October 1977

Department of Civil Engineering
Massachusetts Institute of Technology
Cambridge, Massachusetts

50272-101

REPORT DOCUMENTATION PAGE	1. REPORT NO. NSF/RA-770792	2.	3. Recipient's Accession No. PB298857

4. Title and Subtitle
Covariance Analysis of the Response of Buildings to Earthquake Loading (Seismic Safety of Buildings) Internal Study Report No. 15

5. Report Date
October 1977

6.

7. Author(s)
R. Binder

8. Performing Organization Rept. No.

9. Performing Organization Name and Address
Massachusetts Institute of Technology
Department of Civil Engineering
Cambridge, Massachusetts 02139

10. Project/Task/Work Unit No.

11. Contract(C) or Grant(G) No.
(C)
(G) ENV7619021

12. Sponsoring Organization Name and Address
Engineering and Applied Science (EAS)
National Science Foundation
1800 G Street, N.W.
Washington, D.C. 20550

13. Type of Report & Period Covered

14.

15. Supplementary Notes

16. Abstract (Limit: 200 words)

A procedure for predicting the second movements of the response of an elastic shear-beam building model to earthquake loading is reported. Three major sources of uncertainty in the seismic design of a building are ground motion, structure, and the response of the building, especially the method of analysis. This last problem was investigated on the assumption of known ground motion parameters and the choice of a simplified building model (shear-beam) with deterministic structural properties. A brief discussion of traditional analytical procedures precedes presentation of the Structural Response to Earthquake Loading (CASREL) method. Application of CASREL to classical cases of responses to ground motions involving both simple and complicated cases indicate that this procedure is a useful tool for predicting the second moments of the response of an elastic shear-beam model to earthquake loading. It gives exact results for elastic systems, but it is not satisfactory for computing the responses of inelastic systems. Extensive graphs, equations, and references are included.

17. Document Analysis a. Descriptors

Earthquakes
Earthquake resistant structures
Dynamic structural analysis
Elastic properties
Seismic waves
Design
Covariance
Statistical analysis
Loading
Loads (forces)

b. Identifiers/Open-Ended Terms

Earthquake engineering
Shear-beam model

c. COSATI Field/Group

18. Availability Statement	19. Security Class (This Report)	21. No. of Pages
NTIS		65
	20. Security Class (This Page)	22. Price
		A04A01

(See ANSI-Z39.18) See Instructions on Reverse

OPTIONAL FORM 272 (4-77)
(Formerly NTIS-35)
Department of Commerce

SEISMIC SAFETY OF BUILDINGS

Sponsored by National Science Foundation
Grant ENV 76-19021

INTERNAL STUDY REPORT NO. 15

COVARIANCE ANALYSIS OF THE RESPONSE OF BUILDINGS TO EARTHQUAKE LOADING

by

RICARDO BINDER

Supervised by
Professor J. M. Biggs
Professor E. H. Vanmarcke

October 1977

Department of Civil Engineering
Massachusetts Institute of Technology
Cambridge, Massachusetts

TABLE OF CONTENTS

COVARIANCE ANALYSIS OF THE RESPONSE OF BUILDINGS TO EARTHQUAKE LOADING

INTRODUCTION

The seismic design of a building poses many difficulties to the structural engineer due mainly to the many uncertainties present in the problem. Three major sources of uncertainties are:

- the ground motion: intensity (maximum acceleration), strong motion duration, frequency content (pseudo spectral density function or response spectrum);
- the structure: dynamic properties (natural frequencies), resistances of the structural members, stress-strain relationship of the materials or members;
- the response of the building: model of the building, method of analysis.

This report deals primarily with the third source of uncertainty, specifically with the problem of the method of analysis. We will assume that we know the ground motion parameters and we will choose a simplified model of the building (the shear-beam model) with deterministic structural properties and for that case we will propose a method that has some advantages over the well-known methods of time-history analysis, response spectrum and random vibration. The statement of the problem as well as a brief discussion of the traditional methods are given in Chapter 1. The second chapter presents the theories of covariance analysis and statistical linearization. Finally, in Chapter 3 the proposed method is applied to structures starting with the simplest case (1-story, elastic structure

subjected to white noise support motion) and going to more realistic and complicated cases (multi-degree-of-freedom systems with bilinear hysteretic behavior and subjected to non-white noise motion). Whenever possible the results will be compared with those of other methods. This chapter ends with the general conclusions. After the tables, figures and bibliography, four appendices contain additional information about methods and formulae used in this report.

CHAPTER 1 - STATEMENT OF THE PROBLEM AND METHODS OF ANALYSIS

1.1 Statement of the Problem

Two important steps in the seismic design of a building are the selection of a structural model and the representation of the ground motion.

Structural Model

The most widely used dynamic model for a frame building is the shear beam model (Fig. 1a). In this model the mass of the building is concentrated at each floor level, the floor diaphragms are assumed to be infinitely rigid, and the damping is represented by dashpots connecting each floor with the lower one. The lateral resisting forces of the columns of each floor of the building are added together and assigned to a single spring. Due to these assumptions the response of the model is characterized by one-degree-of-freedom (dof) per floor. The resulting equations of motion are:

for a single-dof system: $$m\ddot{y} + c\dot{y} + F(y) = - m\ddot{u}_g \qquad (1)$$

for a multiple dof system:

$$\begin{aligned} &\text{1st floor} && m_1\ddot{y}_1 + c_1\dot{y}_1 - c_2\dot{y}_2 + F_1(y_1) - F_2(y_2) = - m_1\ddot{u}_g \\ &\text{floor } j \quad 2 \le j < n && m_j a_j + c_j\dot{y}_j - c_{j+1}\dot{y}_{j+1} + F_j(y_j) - F_{j+1}(y_{j+1}) = 0 \\ &\text{floor } n && m_n a_n + c_n\dot{y}_n + F_n(y_n) = 0 \end{aligned} \qquad (2)$$

where: y_i = interstory displacement (floor i relative to floor i-1)

$\dot{y}_i$ = interstory velocity

$\ddot{y}_i$ = interstory acceleration

a_i = absolute acceleration

$\ddot{u}_g$ = ground acceleration at the base of the structure

c_i = damping factor of dashpot connecting floor i with floor i-1

m_i = mass of floor i

$F_i(y_i)$ = restoring force of spring of floor i (Fig. 1.b)

For elastic structures the restoring force is simply given by:

$$F_i(y_i) = k_i y_i$$

where k_i is the stiffness of the spring. In reality, however, the columns of a building do not behave elastically during an earthquake and one has to assume an inelastic behavior for the spring. In this case, a more realistic stress-strain relation is the bilinear hysteretic behavior shown also in Fig. 1.b. The major difficulty in using this relation is that it is not memoryless as is the elastic one. In other words, while the elastic force at any instant of time depends only on the interstory displacement at that instant of time, the restoring force in a bilinear hysteretic model depends on the history of the interstory displacements. Specifically, the stress-strain curve will vary each time the yield level is exceeded. More will be said about this in Section 3.3.

The ground motion

The major uncertainties a structural engineer has to deal with in the dynamic analysis of a building are related to the characterization of the

earthquake ground motion. It was already mentioned that these uncertainties are:

- the intensity
- the frequency content
- the duration.

In relation to the intensity it is important to consider the maximum intensity or peak acceleration as well as the variation in time. Several intensity curves have been suggested by different authors (Fig. 2): trapezoidal curves [1], exponential curves [2], etc. These intensity curves apply as a factor to the maximum amplitude of the motion or to the variance of the acceleration.

The frequency content of the earthquake is very dependent on the origin of the earthquake, the distance epicenter to site, and the soil conditions at the site. Due to this reason it is very unrealistic to take a record of a single earthquake for the dynamic analysis of a structure. Better account of the variability of this parameter is taken by using a response spectra or even better a spectral density function which can be related to the local conditions more easily.

Finally, the duration of the ground motion is also important, especially for flexible structures. Of course it is related to the intensity curve mentioned above. It is most important to define the duration when a constant intensity is assumed as in the traditional random vibration approach. Several authors have given definitions of motion duration [25,26].

1.2 Methods of Analysis

Three types of analysis procedures are of interest. They are: the response spectrum approach, the time history analysis, and the random vibration approach.

The response spectrum approach

It is the simplest way to estimate the maximum system response, say the maximum displacement due to a ground motion. It makes use of the response spectrum which is a plot of the maximum response of single-degree-of-freedom (SDOF) systems for different values of the natural frequency and the damping factor. This response spectrum is of course dependent on the site, reflecting the seismicity of the region and the local soil conditions. For multi-degree-of-freedom (MDOF) systems, the response spectrum is applied to all or only to the lower natural frequencies separately and finally the response is computed from the modal responses with a combination rule (e.g. root-sum-square rule). An extension of this approach for elastoplastic structures has been suggested by Newmark and Hall [27].

The time history analysis

In this method the response is obtained directly from the numerical integration of the equations of motion. For SDOF systems there are two alternative methods: to integrate directly Eq. 1 or to use the Duhamel or convolution integral:

$$X(t) = \int_0^t h(t-\tau)f(\tau)d\tau \qquad (3)$$

where: $h(t-\tau)$ = transfer function

$f(\tau)$ = forcing function (e.g., $\ddot{u}_g(\tau)$,

In both cases the input is a digitalized record of acceleration of real or artificial earthquakes.

For MDOF systems one can perform a modal analysis applying what is done for MDOF systems to each mode and combining the responses, or one can integrate numerically Eqs. 2 without a modal decomposition. When the response

of inelastic systems is required, a modal decomposition cannot be applied. The direct solution of Eqs. 2 instead can be applied to inelastic structures too and has also the advantage that it gives the exact solution (except for round-off errors).

Both methods described so far, the response spectrum approach and the time history analysis, are deterministic. Input data as well as the results are deterministic values. But in view of the uncertainties of the ground motion it is more meaningful to have probabilistic results, e.g. distribution function for the maximum relative displacements. These results can be achieved with deterministic methods by combining the results of a large number of cases or trials all dealing with the same structure but differing in the ground motion.

Monte Carlo Simulation

In a typical Monte Carlo simulation, a large number of artificial earthquakes are generated having some parameters in common, e.g. evolution of the intensity in time, frequency content, whereas others are varied in accordance with a probabilistic law. The structure is subjected to all the earthquakes and a statistical analysis of the responses is performed.

Theoretically, when an infinite number of earthquakes are generated, the resulting probability laws for a given input will be exact. Of course, in practice, this is not possible, and between 20 and 1000 time histories are made. For example, for a gaussian response, 256 trials are necessary to achieve 95% confidence that an accuracy of 10% can be achieved. This large amount of "trials" is the main disadvantage of the Monte Carlo Simulation. It is (economically) justifiable only when no other method is applicable and when the importance of the structure requires an accurate analysis.

Random Vibration Approach

This approach takes into account that the ground motion is of a random nature and determines directly the distribution of the response; specifically, it gives first and second order moments (mean values and variances) of the response from where a distribution function can be constructed. Traditionally this approach works in the frequency domain by defining a spectral density function $G(\omega)$ which contains the information about the frequency content of the earthquakes at a site. The variance of the response and the maximum response for a given probability level can then be computed. For elastic SDOF systems the variance of the relative displacement is given by:

$$\sigma_y^2(t) \simeq \frac{G(\omega_n)}{\omega_n^3}\left(\frac{\pi}{4\beta_t} - 1\right) + \frac{1}{4\omega_n}\int_0^{\omega_n} G(\omega)d\omega \qquad (4)$$

where: $\sigma_y^2(t)$ = variance of the relative displacement at time t

ω_n = natural frequency of the system

β_t = effective damping factor at time t, given by

$$\beta_t = \frac{\beta}{1 - \exp(-2\beta\omega_n t)} \qquad (5)$$

β = critical damping factor

For MDOF systems the variance is computed for each mode separately with the same formula. The variances for the interstory displacements are computed using the modal variances, the modal shape and participation factors. A more detailed explanation of this approach can be found in Ref. [4]. The extension to inelastic structures has also been studied. G. Gazetas [6] proposed a semi-empirical extension of this approach to MDOF elastoplastic systems. It starts with an elastic analysis, defines yielding states depending on which story yields first after each elastic period, computes the

responses for each state independently and finally combines them in accordance with the probability of occurrence of each state. The most important result is the distribution of the ductility factor which can be used directly in a safety analysis.

In the following chapter a state space approach will be presented. It can be regarded as another random vibration approach because it also considers the random nature of the input. Its main difference with the more traditional approach is that it works in the time domain. It has the same advantage of the time history analysis in that it can deal with evolutionary ground motions and that it gives the response at any instant of time during the ground motion. As will be shown, it gives exact solutions for SDOF and MDOF elastic systems. It can also be applied to bilinear hysteretic systems giving reasonable good results for several cases.

Finally, in order to complete the picture about the methods that are being used, a last method should be mentioned. It uses the Fokker-Planck Equation for obtaining the time dependent response statistics. This method is applicable to bi- and trilinear hysteretic SDOF and MDOF structures responding to white noise or filtered ground motion [14,23,24,28].

CHAPTER 2 - COVARIANCE ANALYSIS AND STATISTICAL LINEARIZATION

In this chapter a method will be presented which we will abbreviate by CASREL, which stands for Covariance Analysis of the Structural Response to Earthquake Loading.

2.1 Elastic Structures

The equation of motion for a structure subjected to ground motion (eqs. 1 and 2) can be written as a set of simultaneous first-order differential equations. For SDOF elastic systems Eq. 1 can be written as:

$$\dot{mv} + cv + ky = - m \ddot{u}_g$$

$$v = \dot{y} \tag{6}$$

Defining the state vector $\underline{x}^*$ as $\underline{x} = \begin{Bmatrix} y \\ v \end{Bmatrix}$

Eqs. 6 change to:

$$\dot{\underline{x}} = \begin{bmatrix} 0 & 1 \\ -k/m & -c/m \end{bmatrix} \underline{x} + \begin{Bmatrix} 0 \\ -\ddot{u}_g \end{Bmatrix} \tag{7}$$

The same can be done for MDOF systems (Eqs. 2). For the general case, we will write Eq. 7 in the following way (emphasizing the time dependence):

$$\dot{\underline{x}}(t) = F(t)\, \underline{x}(t) + G(t)\underline{w}(t) \tag{8}$$

where: $F(t)$ and $G(t)$ are continuous time dependent matrices and

$\underline{w}(t)$ is the forcing function vector (ground motion).

In order to consider the randomness of the ground motion, we divide the forcing vector into two components:

---

* A bar underlining a symbol indicates a vector and capital letters symbolize matrices.

$$\underline{w}(t) = \underline{b}(t) + \underline{u}(t)$$

in which $\underline{b}(t) = E[\underline{w}(t)]$ = the mean or expected value and

$\underline{u}(t)$ = the random component, uncorrelated in time (white noise).

Thus, one can write:

$$E[\underline{u}(t)\ \underline{u}^T(\tau)] = Q(t)\ \delta(t-\tau) = \begin{cases} 0 & \text{if } t \neq \tau \\ Q(t) & \text{if } t = \tau \end{cases} \qquad (9)$$

$\delta(t-\tau)$ = Dirac delta, and

$Q(t)$ = the spectral density function at time t.

As a consequence of the random input, the state vector will also have a random component. It can be written as:

$\underline{x}(t) = \underline{m}(t) + \underline{r}(t)$

$\underline{m}(t) = E[\underline{x}(t)]$ = mean value

$\underline{r}(t)$ = random component which in general will be autocorrelated.

A covariance matrix P(t) containing all the second moments of the state variables can be defined as:

$$P(t) = E[\underline{r}(t)\ \underline{r}^T(t)]$$

the element p_{ij} in the i^{th} row and j^{th} column of P is equal to the covariance between the elements i and j of the state vector $\underline{x}$.

Having defined all the components of Eq. 8, it can be written in terms of the mean values and the random components [22]:

$$\dot{\underline{m}}(t) = F(t)\ \underline{m}(t) + G(t)\ \underline{b}(t) \qquad (10a)$$

$$\dot{P}(t) = F(t)\ P(t) + P(t)\ F^T(t) + G(t)\ Q(t)\ G^T(t) \qquad (10b)$$

Eqs. 10 give the propagation of the mean and covariance matrix in time. They can be numerically integrated going in time steps through the time

domain (see Appendix A). Of course, this process can easily be computer coded. The solution is then carried out very efficiently by a computer.

Taking a sample consisting of only one ground motion, Eq. 10a will give the same result as a time history analysis for that ground motion. But in general, a forcing function representative of many earthquakes is taken and then Eq. 10a is identically zero (for zero initial conditions) and Eq. 10b gives the second moments of the state variables. Hence Eqs. 10 provide a direct method for analyzing the statistical properties of the state vector. This is to be contrasted with the Monte Carlo Simulation where many sample trajectories of $\underline{x}$ are calculated from computer-generated random noise. The second moments are then estimated by averaging over the ensemble of generated trajectories. Note also that Eq. 10b leads to exact solutions for P (within computer accuracy) whereas a Monte Carlo Simulation yields only approximate solutions for any finite number of simulations. Consequently, the direct analytical method is both exact and generally the most efficient technique for analyzing linear systems with varying ground motion.

2.2 Statistical Linearization Technique

In order to apply the method described so far to nonlinear systems, a linear approximation for the nonlinearity has to be found first.

For nonlinear systems, Eqs. 1 or 2 can be written in vector form as:

$$\dot{\underline{x}}(t) = \underline{f}(\underline{x},t) + G(t)\,\underline{w}(t) \tag{11}$$

where $\underline{f}(\underline{x},t)$ contains the nonlinear relation between the state variables. We try a linearization of the form:

$$\underline{f}(\underline{x},t) = \hat{\underline{f}} + N(\underline{x}-\underline{m}) \tag{12}$$

The terms of the right-hand side member are computed by imposing the condi-

tions that the error of the approximation defined as:

$$\underline{e} = \underline{f}(\underline{x},t) - \hat{\underline{f}} - N(\underline{x}-\underline{m}) \tag{13}$$

satisfies $E[\underline{e}^T S \underline{e}]$ = minimum for any positive semi-definite matrix S.

For imposing this condition, the joint probability density function (jpdf) of the state variables is required. Since it is in general not available, an exact solution is not possible. One procedure for obtaining an approximate solution is to assume the form of the jpdf of the state variables. Generally the assumption is made that the state variables are jointly Gaussian, because it is convenient, and often reasonable. We will later make different assumptions in order to improve the results, as will be discussed in the next chapter and in Appendix C. It will also be shown there, that the statistical linearization really captures (at least a part) of the nonlinearity of a bilinear hysteretic system. This is a major difference with a Taylor series which loses completely the nonlinearity of that system.

Once $\hat{\underline{f}}$ and N are determined from Eq. 13, the solution of Eq. 11 is carried out in the same way as for elastic systems with following propagation equations:

$$\dot{\underline{m}}(t) = \hat{\underline{f}}(t) + G(t)\ \underline{b}(t) \tag{14a}$$

$$\dot{P}(t) = N(t)\ P(t) + P(t)\ N^T(t) + G(t)\ Q(t)\ G^T(t) \tag{14b}$$

which differ from their elastic counterparts only in that

$F(t)\ \underline{m}(t)$ has been replaced by $\hat{\underline{f}}(t)$ and

$F(t)$ has been replaced by $N(t)$.

Again, we will deal only with Eq. 14b, since Eq. 14a is always zero for zero initial conditions.

2.3 The Spectral Density Function

In the derivation of the differential equations of the covariance matrix P(t), the assumption of uncorrelated forcing function had to be made. This assumption (Eq. 9) leads to the definition of the spectral density function Q(t). In reality it is impossible to have uncorrelated (white noise) ground motion, and a method for avoiding this limitation will be put forth in the next chapter. Moreover, even if we want to impose an ideal white noise, we cannot do it unless we reduce the length of the time steps of the integration procedure to zero. This problem has been discussed already in other publications [7,8]. The autocorrelation function and spectral density function for finite time step lengths are shown in Fig. 3a and b. In Appendix B, a brief analysis shows that for a rectangular psd function the response can be made to be as close to white noise response as desired, by taking the frequency ω_o large enough (Fig. 3c). This means that for the psd function of Fig. 3b, the response will be also as close to white noise as required, provided a sufficiently small Δt is taken.

The relation between this psd function and that generally used in random vibration is:

$$Q(t) = \alpha(t)\,\pi\,G_o$$

CHAPTER 3 - APPLICATIONS OF CASREL

In this chapter the technique described in the previous chapter will be applied to classical cases of responses of structures to ground motions, going from the simple to the more complicated cases. Whenever possible the results will be compared with those of other methods.

3.1 Elastic SDOF Systems Subjected to White Noise Motion

For this simple case, the state vector contains simply the relative displacement and velocity corresponding to the one dof; no linearization has to be performed, and therefore the result is exact (within computer accuracy). This is shown in Table 1, where the results of CASREL for the steady-state variance of the relative displacements are compared with the analytical solution for several values of the natural frequency and the critical damping ratio.

Fig. 4 shows that CASREL can deal with non-stationary ground motions. In 4a the motion starts with full strength at t=0 and stops at t=2 secs. The response shows pretty well the fluctuations due to the transient component and shows very good agreement with the traditional random vibration approach. Fig. 4b shows the response for a smoothly varying ground motion intensity. This is one of the main advantages of CASREL, since other methods (e.g. the response spectrum and stationary random vibration approaches) cannot deal with these cases. Fig. 5 shows the standard deviation of the velocity and the dimensionless coefficient of correlation given by:

$$\rho_{vy} = \frac{Cov(v,y)}{\sigma_v \, \sigma_y}$$

for the same case as Fig. 4b. Both are also direct results of CASREL. An

interesting observation is that the coefficient of correlation tends to zero as the response of the system tends to a steady state .

3.2 Elastic SDOF Systems Subjected to Filtered Ground Motion

As was said in section 8.3, although the input is not rigorously white noise, for practical purposes it can be considered as such when the time step is small. On the other side, ground motions are never white noise, but instead the psd function shows one or more maximum values as shown in Fig. 6 for two records of a real earthquake [5].

There are two ways of dealing with this problem. The first tries to fit a function to the autocorrelation function of the ground motion one wants to reproduce [21]. We prefer and will explain in more detail the second method in which a function is chosen to fit the psd function of the ground motion, because it has more physical meaning. Fig. 7 shows this approach: it is assumed that the structure rests on a soil layer which lies on the bedrock and which filters the white noise motion of the bedrock. The psd function at the base of the structure is given by the transfer function of the soil layer. Generally, the soil layer is considered as a SDOF system with following equation of motion:

$$\ddot{u}_g + 2\xi_g\omega_g\dot{u}_g + \omega_g^2 u_g = -\ddot{u}_r \qquad (16)$$

where u_r and u_g are as defined in Fig. 7 and

ξ_g and ω_g are the equivalent soil damping and frequency. The resulting psd function is the well-known Kanai-Tajimi spectra:

$$G(\omega) = \frac{1 + 4\xi_g^2\left(\frac{\omega}{\omega_g}\right)^2}{\left[1 - \left(\frac{\omega}{\omega_g}\right)^2\right]^2 + 4\xi_g^2\left(\frac{\omega}{\omega_g}\right)^2} G_o \qquad (17)$$

In order to introduce the soil filtering into the covariance analysis, we augment the state vector including two new state variables: u_g and $\dot{u}_g$. Eq. 7 is changed to:

$$\begin{Bmatrix} \dot{u}_g \\ \ddot{u}_g \\ \dot{x} \\ \dot{v} \end{Bmatrix} = \begin{bmatrix} 0 & 1 & 0 & 0 \\ -\omega_g^2 & -2\xi_g\omega_g & 0 & 0 \\ 0 & 0 & 0 & 1 \\ \omega_g^2 & 2\xi_g\omega_g & -k/m & -c/m \end{bmatrix} \begin{Bmatrix} u_g \\ \dot{u}_g \\ x \\ v \end{Bmatrix} + \begin{Bmatrix} 0 \\ -\ddot{u}_r \\ 0 \\ 0 \end{Bmatrix} \qquad (18)$$

Note that since Eq. 18 is applied in time steps, ω_g and ξ_g can be made time-dependent, hence the motion at the base of the structure can be made time dependent in both intensity and frequency content.

Of course, this method can be expanded in order to reproduce psd functions with more than one mode as in Fig. 6b. This is done by writing two or more equations of the type of Eq. 16 for additional state variables. In essence this corresponds to having several horizontal soil layers.

In Table 2 results for the steady-state variance of the relative displacements of CASREL are given for several cases with different natural frequencies and damping ratios of the structure and for two different psd functions which are shown in Fig. 8. These results are compared with those of two methods: the traditional random vibration approach (Eq. 4) and the analytical solution given by Eq. 19 [15].

$$\sigma_y^2 = \frac{\pi G_o}{4\beta\omega_n^3} \frac{\omega_g^4 + \omega_g\omega_n^3(\frac{\beta}{\xi_g}) + 4\omega_g\omega_n[\xi_g\beta(\omega_g^2 + \omega_n^2) + \omega_g\omega_n(\xi_g^2 + \beta^2)]}{(\omega_g^2 - \omega_n^2)^2 + 4\omega_g\omega_n[\xi_g\beta(\omega_g^2 + \omega_n^2) + \omega_g\omega_n(\xi_g^2 + \beta^2)]} \qquad (19)$$

From the results it is clear that in this case CASREL gives also the exact results (within computer accuracy), whereas the traditional random vibration approach has two sources of inaccuracies: Eq. 4 is only approximate (although generally a very good approximation), and furthermore the evaluation of the integral in it will never be exact.

On the other hand, Eq. 4 can be applied to any psd function, whereas CASREL and Eq. 19 require that an approximate Kanai-Tajimi spectra is found first.

3.3 SDOF Inelastic Structures

The statistical linearization as described in section 2.2 has been applied to a great variety of nonlinear systems [16,17]. Applications to bilinear hysteretic systems have been reported by several authors [9,10, 11,12,13,18], sometimes under the names of quasi or equivalent linearizations. In this study a relatively simple linearization was used. A brief explanation follows; the detailed analysis is given in Appendix C.

Fig. 9 shows a decomposition of the bilinear hysteresis (a) into an elastic part (b) and a perfectly elastoplastic part (c). The linearization is applied only to the elastoplastic component introducing a new variable: the plastic displacement d. The assumptions are made that the relative velocity of the system is gaussian distributed, that the restoring force for the elastoplastic system follows a truncated gaussian distribution, and that both are independent.

The result of the analysis is the following linear relation:

$$\begin{Bmatrix} \dot{y} \\ \dot{v} \\ \dot{d} \end{Bmatrix} = \begin{bmatrix} 0 & 1 & 0 \\ -k/m & -2\beta\sqrt{k/m} & k(1-r)/m \\ k\lambda_\phi(1-r) & \lambda_v & k\lambda_\phi(1-r) \end{bmatrix} \begin{Bmatrix} y \\ v \\ d \end{Bmatrix} + \begin{Bmatrix} 0 \\ 0 \\ -\ddot{u}_g \end{Bmatrix} \qquad (20)$$

where

$$\lambda_v = 2p$$

$$\lambda_\phi = \sqrt{\frac{2}{\pi}} \frac{\sigma_v p \phi_m}{\sigma_\phi^2}$$

$$\sigma_\phi^2 = k^2(1-r)^2(\sigma_y^2 + \sigma_d^2 - 2\,\mathrm{Cov}\,(y,d))$$

and p is a function of σ_ϕ/ϕ_m as shown in Fig. 10. It represents the probability of positive (or negative) yielding taking place at an instant of time in which the motion is such that the standard deviation of the restoring force ϕ is σ_ϕ.

Table 3 shows the flow chart for the computations involved in CASREL for the case of an inelastic structure. Although the Runge-Kutta type method requires computation of the linearization coefficients λ_v and λ_ϕ twice for each time step, it does not affect the accuracy of the results to compute them only once.

Of course, the proposed linearization is rather arbitrary. Several other linearizations of the bilinear hysteresis could be found by changing the assumptions or by introducing more state variables (e.g. [13]).

Special cases are those for r = 1.0 (elastic system) and r = 0 (perfectly elastoplastic system). Due to the assumptions explained above for all the values of r unequal to 1.0, CASREL gives only approximate results. How good the approximation is can be assessed only by comparison with Monte Carlo Simulations.

Figs. 11 and 12 show results from 80 simulations (from [18]) and from CASREL. The variance of the relative displacement has been normalized with respect to the paramter D, defined as:

$$D = \sqrt{G_o/\omega_n^3}$$

which is a measure of the intensity of the ground motion with dimensions of length. In both cases the ratio of the secondary to the first stiffness is 1/2. In Fig. 12 the ground motion is stronger than in Fig. 11 for the same structure as indicated by the ratio Δ_y/D (Δ_y= yield displacement).

The fluctuations of the response computed from the simulations for large values of t (e.g., $\omega_n t = 12\pi$) are due to statistical errors and show that an ensemble of 80 simulations is too small. In consequence, it is difficult to assess how well CASREL approximates the exact solution, but the general trend of CASREL is similar to the simulations. What should be emphasized is that in both methods the response tends to a steady-state value even if the damping ratio is zero. This is not true for elastic structures as can be seen easily from Eq. 4.

A better notion about the degree of approximation of CASREL is obtained from Figs. 13 and 14. Here the results of CASREL are compared with Monte Carlo results obtained from 1000 simulations [13]. From these figures it is obvious that the proposed method performs pretty well for rigidity ratios greater than 0.2 or 0.3 (moderate nonlinearity) and for ground motion intensities G_o less than 0.6.

In relation to the effect of the value of r, two points have to be noted: the statistical linearization fails to predict the response for $r \leq 0.1$. Other authors reported this same conclusion even for more compli-

cated linearizations [13,9]. The second interesting point is that the response has a minimum value for r in the neighborhood of 0.3.

With respect to the intensities of the ground motion it should be emphasized that even the lower value of it (G_o = 0.2) produces a pretty high yielding action. This is evident by comparing the steady-state standard deviation of the response for the linear system (for r = 1.0, $\sigma_y = \sqrt{\sigma_y^2} = \sqrt{5} = 2.24$) with the yield displacement (Δy = 1.0) for the bilinear systems. This means that for these systems yielding occurs almost in each oscillation and explains the marked decrease in the response.

Obviously, what was done in order to consider non-stationary or non-white input to linear systems applies also to bilinear systems. Fig. 15 for example shows the responses of an elastic system and of a bilinear hysteretic system (with r = 0.3) to the same nonstationary white noise ground motion.

3.4 Multi-Degree-Of-Freedom Systems

The extension of CASREL to MDOF systems is obvious: the state vector is augmented to contain the relative displacement, the relative velocity and the plastic displacement (for inelastic systems) for each floor. The matrix N(t) is obtained after some algebraic manipulations from Eqs. 2 and is given in Table 3. In the remaining aspects the procedure outlined for SDOF systems can be applied in the same way.

Fig. 16 shows the response for an elastic 4 DOF system with the characteristics shown in Table 5 to stationary and filtered ground motion. For comparison, the results of the random vibration approach in the frequency domain are given. For doing this the damping coefficients were taken propor-

tional to the corresponding stiffnesses in order to be able to decouple the modal equations of motion. This is necessary because the random vibration approach in the frequency domain works with modal equations (and dampings; see Appendix D).

In Fig. 17 the responses of an elastic system and an inelastic system with the same natural (small amplitude) frequency and subjected to the same non-stationary ground motion are shown. No comparison with other methods are possible in these cases.

General Conclusions

The procedure outlined in Chapters 2 and 3 represents a powerful tool for predicting the second moments of the response of an elastic shear beam model to earthquake loading.

As was shown, it gives exact results for elastic single and multi-degree of freedom systems and for white noise or filtered ground motion. In these cases its main advantages are:

- it treats ground motion and response in a probabilistic manner, giving directly the second moments of the response;

- it deals very easily with time varying ground motions in intensity as well as frequency content.

However, our main objective in trying this procedure was to compute the responses of inelastic systems. From comparisons with Monte-Carlo simulations we have to conclude that for these systems the results are not satisfactory for the particular linearization used. It also seems doubtful that other statistical linearizations would do much better for bilinear hysteretic systems with low secondary stiffnesses ($r < 0.2$).

TABLE 1 - RESULTS FOR ELASTIC SINGLE-DEGREE-OF-FREEDOM SYSTEMS SUBJECTED TO WHITE NOISE INPUT

Natural Frequency	Critical Damping	$\sigma_x^2 = \pi G_o / 4\beta\omega_n^3$	CASREL
5	0.05	0.12566	0.12566
10	0.05	0.015708	0.015708
15	0.05	0.004654	0.004654
20	0.05	0.001963	0.001964
10	0.02	0.039270	0.03927
10	0.10	0.007854	0.007854

TABLE 2 - RESULTS FOR ELASTIC SINGLE-DEGREE-OF-FREEDOM SYSTEMS SUBJECTED TO FILTERED MOTION

Ground Frequency	Ground Damping	Natural Frequency	Critical Damping	Analytical Result (Eq. 19)	Random Vibration (Eq. 4)	CASREL
15	0.7	10	0.02	0.061534	0.0620	0.06153
		10	0.05	0.024193	0.0243	0.02419
	0.4	5	0.05	0.15588	0.1558	0.15588
		10	0.05	0.03267	0.0331	0.03267
		20	0.05	0.00262	0.00248	0.00262

TABLE 3 - FLOW CHART OF CASREL FOR INELASTIC STRUCTURES

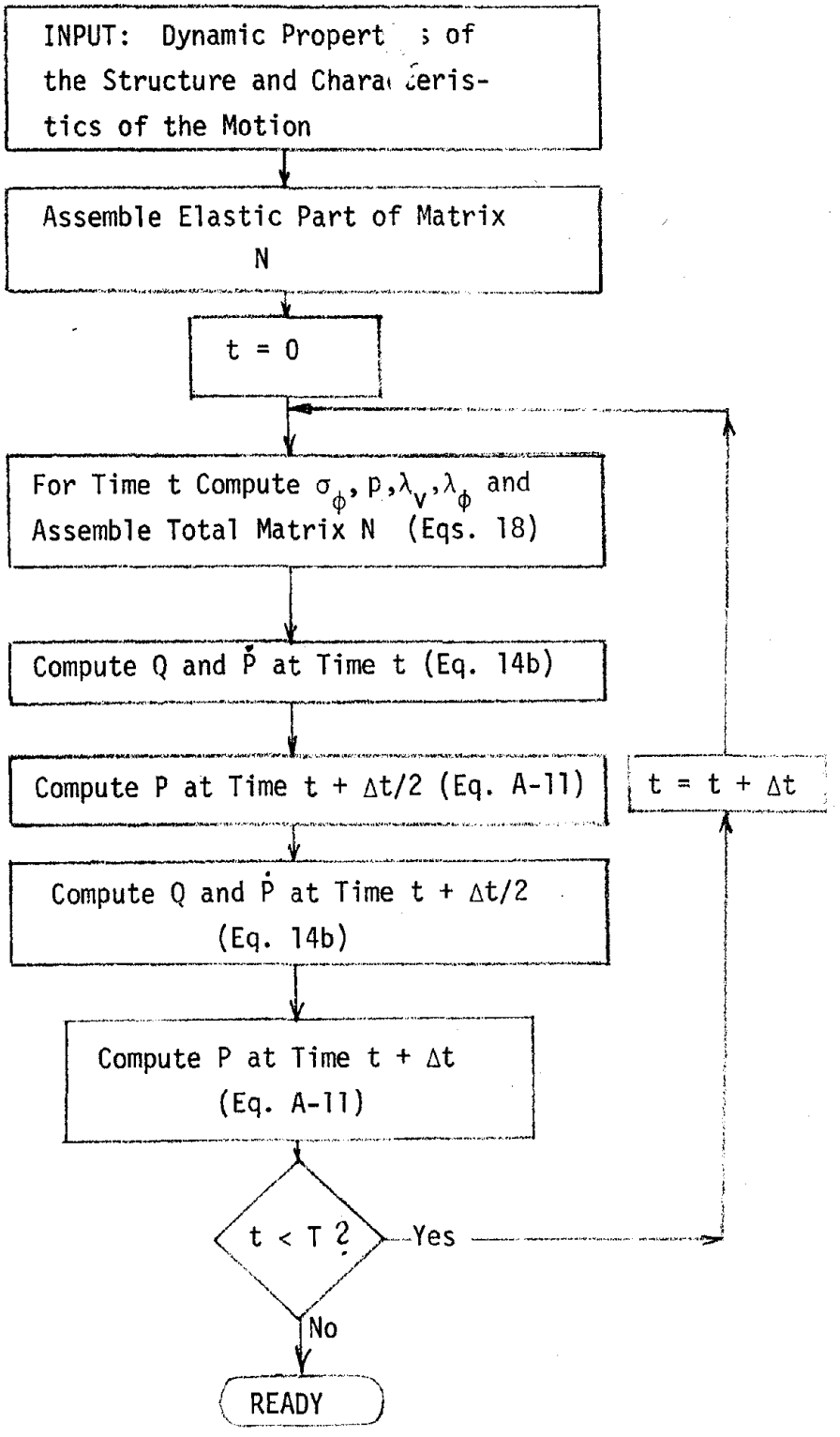

TABLE 4 - Equation 8 for an Inelastic Structure with n Degrees-of-Freedom

$$
\begin{Bmatrix} \dot{U}_g \\ \ddot{U}_g \\ \ddot{y}_1 \\ \ddot{y}_1 \\ \dot{d}_1 \\ \dot{y}_2 \\ \ddot{y}_2 \\ \dot{d}_2 \\ \dot{y}_3 \\ \vdots \\ \dot{y}_{n-1} \\ \ddot{y}_{n-1} \\ \dot{d}_{n-1} \\ \dot{y}_n \\ \ddot{y}_n \\ \dot{d}_n \end{Bmatrix} =
\begin{bmatrix}
 & 1.0 & & & & & & & & & & & & & \\
-\omega_g^2 & -2\xi_g\omega_g & & & & & & & & & & & & & \\
 & & & 1.0 & & & & & & & & & & & \\
\omega_g^2 & 2\xi_g\omega_g & -A_1 & -B_1 & A_1C_1 & A_2\mu_2 & B_2\mu_2 & -A_2C_2\mu_2 & & & & & & & \\
 & & \lambda\phi_1 K_1 C_1 & \lambda v_1 & -\lambda\phi_1 K_1 C_1 & & & & & & & & & & \\
 & & & & & 1.0 & & & & & & & & & \\
 & & A_1 & B_1 & -A_1C_1 & -A_2D_2 & -B_2D_2 & A_2C_2D_2 & k_3\mu_3 & B_3\mu_3 & -A_3C_3\mu_3 & & & & \\
 & & & & & \lambda\phi_2 K_2 C_2 & \lambda v_2 & -\lambda\phi_2 K_2 C_2 & & & & & & & \\
 & & & & & & & & 1.0 & & & & & & \\
 & & & & & & & & & & & & & & \\
 & & & & & & & & & 1.0 & & & & & \\
 & & & & & & & & -A_{n-1}D_{n-1} & -B_{n-1}D_{n-1} & A_{n-1}C_{n-1}D_{n-1} & A_n\mu_n & B_n\mu_n & -A_nC_n\mu_n & \\
 & & & & & & & & \lambda\phi_{n-1}K_{n-1}C_{n-1} & \lambda v_{n-1} & -\lambda\phi_{n-1}K_{n-1}C_{n-1} & & & & \\
 & & & & & & & & & & & 1.0 & & & \\
 & & & & & & & & A_{n-1} & B_{n-1} & -A_{n-1}C_{n-1} & -A_nD_n & B_nD_n & A_nC_nD_n & \\
 & & & & & & & & & & & \lambda\phi_n K_n C_n & \lambda v_n & -\lambda\phi_n K_n C_n &
\end{bmatrix}
\begin{Bmatrix} U_g \\ \dot{U}_g \\ y_1 \\ \dot{y}_1 \\ d_1 \\ y_2 \\ \dot{y}_2 \\ d_2 \\ y_3 \\ \vdots \\ y_{n-1} \\ \dot{y}_{n-1} \\ d_{n-1} \\ y_n \\ \dot{y}_n \\ d_n \end{Bmatrix} +
\begin{Bmatrix} 0 \\ -\ddot{u}_r \\ 0 \\ 0 \\ 0 \\ 0 \\ 0 \\ 0 \\ 0 \\ \vdots \\ 0 \\ 0 \\ 0 \\ 0 \\ 0 \\ 0 \end{Bmatrix}
$$

Elements not shown are zero. $\mu_i = \frac{m_i}{m_{i-1}}$; $A_i = \frac{k_i}{m_i}$ $B_i = \frac{c_i}{m_i}$ $C_i = 1 - r_i$ $D_i = 1 + \mu_i$

TABLE 5 - PROPERTIES OF THE 4-DOF SYSTEM

Story	Mass	Primary Stiffness	Resist-ance	Yield Dis-placement	Damping Factor
1	0.5	127.8	4.142	0.0324	0.9192
2	0.5	127.8	3.643	0.0285	0.9192
3	0.5	127.8	2.704	0.0212	0.9192
4	0.5	127.8	1.439	0.01126	0.9192

Modal Properties			Modal Shapes			
Mode	Frequency	Damping Ratio	Floor 1	Floor 2	Floor 3	Floor 4
1	5.56	0.02	1.00	1.88	2.53	2.88
2	16.00	0.058	1.00	1.00	0.00	-1.00
3	24.51	0.088	1.00	-0.35	-0.88	0.65
4	30.07	0.108	1.00	-1.53	1.35	-0.53

Units are in kips, ft, sec.

Bibliography

1. Hou, S., "Earthquake Simulation Models and Their Applications," MIT Dept. of Civil Engineering, Report R68-17, May 1968,

2. Saragoni and Hart, "Simulation of Artificial Earthquakes," International Journal of Earthquake Engineering, Structural Dynamics, Vol. 2, No. 3, 1974.

3. Shinozuka, M., "Digital Simulation of Ground Acceleration," Proceedings 5th WCEE, Rome, Italy, June 1973.

4. Vanmarcke, Erik H., "Structural Response to Earthquakes," Chapter 8 from Seismic Risk and Engineering Decisions, C. Lomnitz and E. Rosenblueth, Editors, Elsevier Publ., 1976.

5. Shih-Chi Liu, "Autocorrelation and Power Spectral Density Functions of the Parkfield Earthquake of June 27, 1966," Bulletin of the Seismological Society of America, Vol. 59, No. 4, Aug. 1969.

6. Gazetas, George, "Random Vibration Analysis of Inelastic Multi-Degree-of-Freedom Systems Subjected to Earthquake Ground Motion, Ph.D. Thesis, August 1976, M.I.T. Dept. of Civil Engineering.

7. Cook, R. Gordon, "Digital Simulation of Random Vibrations," Ph.D. Thesis, MIT Dept. of Mechanical Engineering, 1964.

8. Yanev, Peter, "Response of Simple Inelastic Systems to Random Excitation, Ph.D. Thesis, MIT Dept. of Civil Engineering, June 1970.

9. Caughey, Tomas K., "Equivalent Linearization Technique," The Journal of the Acoustical Society of America, Vol. 35, No. 1, Nov. 1963.

10. Lutes, Loren D., "Stationary Random Response of Bilinear Hysteretic Systems " EERL, CALTECH, Pasadena, California 1967.

11. Iwan, W.D. and Lutes, L.D., "The Response of the Bilinear Hysteretic System to Stationary Random Excitation," Journal of the Acoustical Society of America, Vol. 43, No. 3, March 1968.

12. Lutes, Loren D., "Equivalent Linearization for Random Vibration," Journal of the Engineering Mechanics Div., ASCE, June 1970.

13. Kobori, T., Minai, R., and Suzuki, Y., "Statistical Linearization Techniques for Dynamical Systems with Fluctuating Hysteresis," Theoretical and Applied Mechanics, Vol. 23, Procced. of the 23rd Japan National Congress for Applied Mech., 1973.

14. Kobori, T., Minai, R., and Suzuki, Y., "Stochastic Seismic Response of Hysteretic Structures," Bulletin of the Disaster Prevention Res. Inst., Kyoto Univ., Vol. 26, Part 1, No. 236, March 1976.

15. Crandall, S.H. and Mark, W.D., Random Vibration in Mechanical Systems, Academic Press, New York, 1963.

16. TASC (The Analytic Sciences Corporation), The Covariance Analysis Describing Function Technique" (Cadet).

17. Gelb, A. and Van der Velde, W.E., Multiple-Input Describing Functions and Nonlinear System Design, McGraw-Hill Book Co., New York 1968.

18. Lutes, L. and Shah, V., "Transient Random Response of Bilinear Oscillators," Report No. 17, Dept. of Civil Engineering, Rice University, Houston, Texas, Dec. 1972.

19. Crandall, Engineering Analysis, McGraw-Hill, 1956.

20. Bathe, K.J. and Wilson, E.L., Numerical Methods in Finite Element Analysis, Prentice-Hall, Inc., New Jersey, 1976.

21. Gelb, A., Automatic Control, MIT Press 1974.

22. Jazwinsky, A.H., Stochastic Processes and Filtering Theory, Academic Press, Inc., New York, 1970.

23. Kobori, T., Minai, R., and Asano, K., "Random Response of the Nonlinear System with Hysteretic Characteristics," Theoretical and Applied Mechanics, Vol. 24, 1974.

24. Asano, K., Suzuki, S., "Study on Nonlinear Hysteretic Response of a Single- and Multi-Storeyed Building Structures to Random Excitation," Technology Reports of Kansai University, No. 17, November 1975.

25. Trifunac, M.D. and Brady, A.G., "A Study of the Duration of Strong Earthquake Ground Motion," Bulletin of the Seismological Society of America, Vol. 65, No. 3

26. Vanmarcke, Erik H., and Lai, Shish-sheng P., "Strong Motion Duration of Earthquakes," M.I.T. Dept. of Civil Engineering Research Report R77-16, Order No. 569, July 1977.

27. Newmark and Hall, "Seismic Design Criteria for Nuclear Reactor Facilities," Proceed. 5th WCEE, Rome, Italy, June 1973.

28. Wong, Ming Chen and Uhlenbeck, G.E., "On the Theory of the Brownian Motion II," Review of Modern Physics, Vol. 17, 1945.

29. Husid, R., Medina, H. and Rios, J., "Análisis de Terremotos Norteamericanos y Japoneses," Revista del IDIEM, 8, 1969, Santiago, Chile.

APPENDIX A - STABILITY OF THE INTEGRATION METHODS

One of the major problems to be solved when a procedure with numerical integration is to be used is the selection of the appropriate integration method. This method must be simple, accurate and stable. There are a large number of methods (see for example [19]) with different degrees of complexity. Here, only three widely used methods will be discussed: the Forward Step or Euler method, the central difference method (CDM) and a Runge-Kutta type method (RKTM).

First a comment about the order of the differential equations involved in our problem is necessary. In Chapter 2/the following differential equations were obtained for elastic structures:

$$\dot{\underline{m}}(t) = F(t)\,\underline{m}(t) + G(t)\,\underline{b}(t) \qquad \text{(A-1)}$$

$$\dot{P}(t) = F(t)\,P(t) + P(t)\,F^{T}(t) + G(t)\,Q(t)\,G^{T}(t) \qquad \text{(A-2)}$$

For inelastic structures, once the linearization has been performed, the analysis is completely similar except that N(t) replaces F(t). Eq. A-1 is a second-order differential equation. In consequence, for that equation the Euler method is conditionally stable (condition: $\Delta t \leq 1/\pi\omega_n$, where Δt is the time step and ω_n the highest natural frequency of the system), and both the CDM and the RKTM are unconditionally stable.

However, we are interested in Eq. A-2, which is a third-order differential equation. This can be shown as follows: For the simplest case (elastic SDOF system, white noise ground motion), Eq. A-2 can be written as:

$$\frac{\partial}{\partial t}\begin{bmatrix}\mathrm{Var}(y) & \mathrm{Cov}(y,v)\\ \mathrm{Cov}(y,v) & \mathrm{Var}(v)\end{bmatrix} = \begin{bmatrix}0 & 1\\ -k/m & -2\beta\sqrt{k/m}\end{bmatrix}\begin{bmatrix}\mathrm{Var}(y) & \mathrm{Cov}(y,v)\\ \mathrm{Cov}(y,v) & \mathrm{Var}(v)\end{bmatrix} +$$

$$+ \begin{bmatrix}\mathrm{Var}(y) & \mathrm{Cov}(y,v)\\ \mathrm{Cov}(y,v) & \mathrm{Var}(v)\end{bmatrix}\begin{bmatrix}0 & -k/m\\ 1 & -2\beta\sqrt{k/m}\end{bmatrix} + \begin{bmatrix}0 & 0\\ 0 & \mathrm{Var}\,(\ddot{u}g)\end{bmatrix} \qquad (A.3)$$

Eliminating the terms in v we get the following equation, in which $Z = \mathrm{Var}(y)$

$$\frac{\partial^3}{\partial t^3} Z + 6\beta\sqrt{k/m}\ \frac{\partial^2}{\partial t^2} Z + 4\,\frac{k}{m}\,(1 + 2\beta^2)\,\frac{\partial}{\partial t} Z + 8\beta\sqrt{(k/m)^3}\ Z = \mathrm{Var}\,(\ddot{u}g) \qquad (A.4)$$

Eq. A-4 is clearly a third-order differential equation in Z. It will control the stability of the integration method.

The stability can be checked by writing the variables at time $t+\Delta t$ as a function of their values at time t in matricial form:

$$\underline{Z}_{t+\Delta t} = A\,\underline{Z}_t + B\,\underline{f}_t + C\,f_{t+\Delta t} \qquad (A.5)$$

where $\underline{Z}_t$ contains the variables at time t and $\underline{f}_t$ is the forcing function at time t.

Since this equation is applied in a recursive way for many time steps, an error in $\underline{Z}_t$ should not increase when computing $\underline{Z}_{t+\Delta t}$. For this to happen, the eigenvalues of the matrix A must be in absolute value less than one [20]. This condition leads generally to a limitation in the length of the time step Δt that can be chosen. Three situations may arise:

1. There is no value of Δt that satisfies the condition. The method is unstable.
2. There is a finite interval of values for Δt that satisfy the condition. The method is conditionally stable.

3. Any value of Δt may be chosen. The method is unconditionally stable.

We will check the stability of the three methods mentioned above.

The Euler Method

The basic equation of the Euler method is:

$$X_{t+\Delta t} = X_t + \Delta t\, \dot{X}_t \tag{A-6}$$

If this equation is applied to the covariance matrix P and substituting from Eq. A-2, the following equation is obtained:

$$\begin{Bmatrix} \mathrm{Var}(y) \\ \mathrm{Cov}(y,v) \\ \mathrm{Var}(v) \end{Bmatrix}_{t+\Delta t} = \begin{bmatrix} 1 & 2\Delta t & 0 \\ -\frac{k}{m}\Delta t & (1-2\beta\sqrt{\frac{k}{m}}\,\Delta t & \Delta t \\ 0 & -\frac{2k}{m}\Delta t & 1-4\beta\sqrt{\frac{k}{m}}\,\Delta t \end{bmatrix} \begin{Bmatrix} \mathrm{Var}(y) \\ \mathrm{Cov}(y,v) \\ \mathrm{Var}(v) \end{Bmatrix}_t + \begin{Bmatrix} 0 \\ 0 \\ \Delta t\ \mathrm{Var}(\ddot{u}g) \end{Bmatrix}_t \tag{A-7}$$

Eq. A-7 is of the same form as Eq. A-5, in which

$$A = \begin{bmatrix} 1 & 2\Delta t & 0 \\ -\frac{k}{m}\Delta t & (1-2\beta\sqrt{\frac{k}{m}}\,\Delta t) & \Delta t \\ 0 & -2\frac{k}{m}\Delta t & 1-4\beta\sqrt{\frac{k}{m}}\,\Delta t \end{bmatrix} \tag{A-8}$$

The eigenvalues λ of A are obtained by equating the determinant of $A-\lambda I$ to zero. The characteristic polynomial obtained in such a way is:

$$\lambda^3 + \lambda^2(6\beta\omega\Delta t-3)+\lambda(12\omega^2\Delta t^2 - 10\beta\omega\Delta t+3)+ 8\beta\omega^3\Delta t^3$$

$$- 4\omega^2\Delta t^2(2\beta^2+1) + 6\beta\omega\Delta t-1 = 0 \tag{A-9}$$

The solutions for λ are:

$$\lambda_1 = 1 - 2\beta\omega\Delta t$$

$$\lambda_2 = 1 - 2\beta\omega\Delta t - 2\omega\Delta t\, i\sqrt{1-\beta^2}$$

$$\lambda_3 = 1 - 2\beta\omega\Delta t + 2\omega\Delta t\, i\sqrt{1-\beta^2}$$

Imposing the condition that the absolute values of the eigenvalues λ are less than 1, the condition obtained is:

$$\omega\Delta t < \beta$$

Since this condition implies very small time steps and hence high computer costs, other integration methods have to be investigated.

The Central Difference Method

The basic equation for the CDM is:

$$X_{t+\Delta t} = X_{t-\Delta t} + 2\Delta t\, \dot{X}_t \qquad \text{(A-10)}$$

In a similar way as for the Euler method it can be shown that the CDM is also unstable, except for very small time steps.

The Runge-Kutta Type Method

The RKTM works with the time derivative and function at half time steps. The equations are:

$$X_{t+\frac{1}{2}\Delta t} = X_t + \frac{\Delta t}{2}\dot{X}_t \qquad \text{(A.11)}$$

$$X_{t+\Delta t} = X_t + t\,\dot{X}_{t+\frac{1}{2}\Delta t}$$

Combining Eq. A-11 with Eq. A-2, one obtains:

$$\begin{Bmatrix} \text{Var}(y) \\ \text{Cov}(y,v) \\ \text{Var}(v) \end{Bmatrix}_{t+\Delta t} = \begin{bmatrix} 1-\omega^2\Delta t & \Delta t^2 & 2(1-\beta\omega\Delta t)\Delta t \\ \Delta t\omega^2(\beta\omega\Delta t-1) & (1-3\beta\omega\Delta t)\Delta t & -2(1-\beta^2)\omega^2\Delta t^2-2\beta\omega\Delta t+1 \\ \Delta t^2\omega^4 & (8\beta^2\Delta t^2\omega^2-\omega^2\Delta t^2-4\beta\omega\Delta t+1 & (6\beta\omega^3\Delta t^2-2\omega^2\Delta t) \end{bmatrix}$$

$$\begin{Bmatrix} \text{Var}(y) \\ \text{Cov}(y,v) \\ \text{Var}(v) \end{Bmatrix}_t + \begin{Bmatrix} 0 \\ \Delta t\ \text{Var}\,\ddot{u}g \\ 0 \end{Bmatrix}_{t+\frac{1}{2}\Delta t} + \begin{Bmatrix} 0 \\ -2\omega\Delta t^2\ \text{Var}(\ddot{u}g) \\ \frac{\Delta t^2}{2}\ \text{Var}(\ddot{u}g) \end{Bmatrix}_t$$

(A.12)

The characteristic polynomial of matrix A is now:

$$\lambda^3+\lambda^2(2\omega^2\Delta t^2(2-5\beta^2)+ 6\beta\omega\Delta t-3)+\lambda(4\omega^4\Delta t^4(4\beta^4-2\beta^2+1)- 24\beta^3\omega^3\Delta t^3-4\omega^2\Delta t^2(1-7\beta^2)$$
$$-12\beta\omega\Delta t-3) - 8\beta^2\omega^6\Delta t^6 + 8\beta\omega^5\Delta t^5(1+2\beta^2) - 4\omega^4\Delta t^4(1+4\beta^2+4\beta^4) +8\beta\omega^3\Delta t^3(1+3\beta^2)$$
$$- 18\beta^2\omega^2\Delta t^2 + 6\beta\omega\Delta t-1 = 0 \qquad \text{(A-13)}$$

The solutions to Eq. A-13 are:

$$\begin{aligned}
\lambda_1 &= 2\beta^2\omega^2\Delta t^2 - 2\beta\omega\Delta t + 1 \\
\lambda_2 &= 2\omega^2\Delta t^2(2\beta^2-1)- 2\beta\omega\Delta t+1 + 2i\sqrt{1-\beta^2}\ \omega\Delta t(2\beta\omega\Delta t - 1) \\
\lambda_3 &= 2\omega^2\Delta t^2(2\beta^2-1)- 2\beta\omega\Delta t+1 - 2i\sqrt{1-\beta^2}\ \omega\Delta t(2\beta\omega\Delta t - 1)
\end{aligned} \qquad \text{(A-14)}$$

Imposing the condition that the absolute values of the eigenvectors are less than one, the following inequalities are obtained:

$$\begin{gathered}
\omega^3\Delta t^3 - 2\beta\omega^2\Delta t^2 + 2\beta^2\omega\Delta t - \beta < 0 \\
\beta\omega\Delta t < 1
\end{gathered} \qquad \text{(A-15)}$$

The maximum values for $\omega\Delta t$ for different damping ratios are:

β	$(\omega\Delta t)_{max}$
0.01	0.22
0.02	0.28
0.05	0.40
0.07	0.45
0.10	0.52

In consequence, this RKTM is also conditionally stable. The limitation on the maximum value for the time step is of little importance for SDOF systems, but may become troublesome for MDOF systems for which the condition must be satisfied by all and in particular by the largest natural frequency.

To avoid this limitation, more complicated integration methods (e.g. of the Runge-Kutta family) would have to be used.

Figs. A-1 and A-2 show the displacement response of a SDOF system calculated with the three methods and for two different time step lengths. It can be seen that in both the Euler method is clearly unstable; the same is true for the CDM (which in Fig. A-2 is fluctuating very slightly at 12 secs) and that in both the RKTM is stable since the condition is satisfied.

APPENDIX B

THE EFFECT OF THE PSEUDO-SPECTRAL-DENSITY FUNCTION ON THE RESPONSE

The analytical solution for the variance of the relative displacement of a SDOF system subjected to a motion characterized by the pseudo spectral density function shown in Fig. B-1a is given by the following equation [15]:

$$\sigma_y^2 = \frac{\pi G_o}{4\beta\omega_n^3}\left[I(\omega_2/\omega_n,\beta) - I(\omega_1/\omega_n,\beta)\right] \tag{B-1}$$

where

$$I(\omega_i/\omega_n,\beta) = \frac{1}{\pi}\,\text{arc tg}\left[\frac{2\beta(\omega_i/\omega_n)}{1-(\omega_i/\omega_n)^2}\right] + \frac{\beta}{2\pi\sqrt{1-\beta^2}}\,\ell n\,\frac{1+(\omega_i/\omega_n)^2+2\sqrt{1-\beta^2}\,(\omega_i/\omega_n)}{1+(\omega_i/\omega_n)^2-2\sqrt{1-\beta^2}\,(\omega_i/\omega_n)} \tag{B-2}$$

β = critical damping ratio of the system

ω_n = natural frequency of the system

ω_1, ω_2 and G_o are parameters of the psd function (Fig. B-1a).

A plot of $I(\omega_i/\omega_n,\beta)$ is shown in Fig. B-2.

If we make $\omega_1 = 0$ and $\omega_2 = \infty$ in Eqs. B-1 and B-2, we get:

$$\sigma_y^2 = \frac{\pi G_o}{4\beta\omega_n^2}$$

the response for white noise. Thus,

$$\frac{\sigma_y^2}{\frac{\pi G_o}{4\beta\omega_n^3}} = I(\omega_2/\omega_n,\beta) - I(\omega_1/\omega_n,\beta) \tag{B-3}$$

represents the ratio of the response to a psd function as in Fig. B-1a to the white noise response.

We are particularly interested in the case when $\omega_1 = 0$ and $\omega_n \leq \omega_2 < \infty$ (Fig. B-1b). For this case:

$$I(\omega_1/\omega_n, \beta) = 0$$

$$\frac{\frac{\sigma_y^2}{\pi G_0}}{4\beta\omega_n^3} = I(\omega_2/\omega_n, \beta) \qquad \text{(B-4)}$$

As can be seen from Fig. B-2, this ratio is very close to unity when ω_2 is higher than ω_n. For example, for $\beta < 0.05$ and $\omega_2 = 1.5\omega_n$, the response differs from the white noise response in less than 1%. So, by choosing ω_2 large enough, we can make the response of the system to the psd function of Fig. B-1b as close to the response to white noise as desired.

APPENDIX C - A STATISTICAL LINEARIZATION FOR BILINEAR HYSTERETIC SYSTEMS

The bilinear hysteretic restoring force is shown in Fig. 9a. Figs. 9b and9c show a decomposition of the original restoring force into two parts: an elastic component and an elastoplastic component. The equation of the decomposition is:

$$F(y) = Kry + \phi(y) \tag{C-1}$$

The elastic component can be entered directly into Eq. 7. The second component, however, requires further study. First we introduce a new variable, the plastic displacement d. The definition of d is given by the following relations:

$$\dot{d} = \begin{cases} v & \text{if } \begin{cases} \phi = \phi_m & \text{and } v > 0 \\ \phi = -\phi_m & \text{and } v < 0 \end{cases} \\ 0 & \text{elsewhere} \end{cases} \tag{C-2}$$

Due to this definition, we can write:

$$\phi(y) = K(1-r)(y-d) \tag{C-3}$$

Now, all we have to find is a linear relation of $\dot{d}$ with the other state variables. Since the definition of d evidences a marked dependence of $\dot{d}$ on v and ϕ, we can try a linearization of the type

$$\dot{d} = \lambda_v \, v + \lambda_\phi \cdot \phi \tag{C-4}$$

where λ_v and λ_ϕ are parameters to be determined by minimizing the error e:

$$e = \dot{d} - \lambda_v \, v - \lambda_\phi \, \phi \tag{C-5}$$

The mean square error is:

$$E(e^2) = E(\dot{d}^2) + \lambda_v^2 E(v^2) + \lambda_\phi^2 E(\phi^2) + 2\lambda_v\lambda_\phi E(v\phi) - 2\lambda_v\lambda_\phi E(v\phi) - 2\lambda_v E(\dot{d}v) - 2\lambda_\phi E(\dot{d}\phi) \tag{C-6}$$

where E means expectation or mean value.

Imposing the minimum error condition, we get:

$$\frac{\partial}{\partial\lambda_v} E(e^2) = 2\lambda_v E(v^2) + 2\lambda_\phi E(v\phi) - 2E(\dot{d}v) = 0$$
$$\frac{\partial}{\partial\lambda_\phi} E(e^2) = 2\lambda_\phi E(\phi^2) + 2\lambda_v E(v\phi) - 2E(\dot{d}\phi) = 0 \qquad \text{(C-7)}$$

From these equations we have to obtain expressions for λ_v and λ_ϕ. From statistics and in view of Eq. C-3, we know that

$$E(\phi^2) = \sigma_\phi^2 = K^2(1-r)^2 (\sigma_y^2 + \sigma_d^2 - 2 \text{ Cov } (y,d)) \qquad \text{(C-8)}$$

and $$E(v^2) = \sigma_v^2$$

Expressions for the covariances $E(v\phi)$, $E(\dot{d}v)$ and $E(\dot{d}\phi)$ can be obtained only by making assumptions about the probability density functions of ϕ and v. Since ϕ can take values only in the interval $(-\phi_m,\phi_m)$ and there is a finite probability that $\phi = \phi_m$ or $\phi = -\phi_m$ at any instant of time, we will assume that the probability distribution of ϕ is a truncated gaussian distribution as shown in Fig. C-1.[1] Furthermore, and for simplicity, we will assume that the velocity is gaussian distributed and that ϕ and v are independent. Only the results can tell how good these assumptions are.

With these assumptions, we are able to compute the covariances in the following way:

$$E(v\phi) = 0 \quad \text{(due to the independence assumption)}$$
$$E(\dot{d}v) = \int_{-\infty}^{\infty}\int_{-\infty}^{\infty} f_{\dot{d}v}(u,w)u \, du \quad wdw \qquad \text{(C-9)}$$

where $f_{\dot{d}v}(u,w) = P_r(u \leq \dot{d} < u + du, w \leq v < w + dw)$

Due to the definition of d, there are two alternatives:

$$\begin{cases} \dot{d} = v & \text{if } \phi = \phi_m \quad \text{or } \phi = -\phi_m \text{ with probability } 2p \\ \dot{d} = 0 & \text{otherwise.} \end{cases}$$

and the joint probability density of $\dot{d}$ and v is given by:

$$\int_{-\infty}^{\infty} u f_{\dot{d}\,v}(u,w)du = \begin{cases} 0 & \text{if } u \neq w \\ 0 & \text{if } u = w \text{ and } -\phi_m < \phi < \phi_m \\ w f_v(w) & \text{if } u = w \text{ and } \phi = \phi_m \text{ or } \phi = -\phi_m \\ & \quad \text{with probability } 2p \end{cases} \tag{C-10}$$

$$E(\dot{d}v) = 2p \int_{-\infty}^{\infty} w^2 f_v(w)dw$$

$$E(\dot{d}v) = 2p\,\sigma_v^2 \tag{C-11}$$

$$E(\dot{d}\phi) = \int_{-\infty}^{\infty}\int_{-\infty}^{\infty} uw\, f_{\dot{d}\phi}(u,w)du\,dw \tag{C-12}$$

$$f_{\dot{d}\phi}(u,w) = Pr(u \leq \dot{d} < u + du,\ w \leq \phi < w + dw)$$

$$\dot{d} = 0 \quad \text{if } \phi \neq -\phi_m \text{ and } \phi \neq \phi_m$$

$$\dot{d} = v \quad \text{if } \phi = -\phi_m \text{ or } \phi = \phi_m$$

$$wuf_{\dot{d}\phi}(u,w) = \begin{cases} 0 & \text{if } |w| \neq \phi_m \\ uf_v(u)\,\phi_m & \text{if } |w| = \phi_m \text{ (with probability } 2p) \end{cases} \tag{C-13}$$

Introducing C-13 into C-12 we have:

$$E(\dot{d}\phi) = \int_{-\infty}^{\infty} \frac{1}{\sqrt{2\pi}\sigma_v} e^{-\frac{u^2}{2\sigma_v^2}}\, udu\, 2p\,\phi_m$$

$$= \sqrt{2/\pi}\,\sigma_v p\,\phi_m \tag{C-14}$$

Finally, from Eqs. C-7, C-11 and C-14, we get:

$$\lambda_v = 2p \tag{C-15}$$

$$\lambda_\phi = \frac{\sqrt{2/\pi}\,\sigma_v p \phi_m}{\sigma_\phi^2}$$

All that is left is to relate p and σ_ϕ. This can be done by imposing the fundamental conditions of probability and other known conditions to the distribution of ϕ shown in Fig. C-1.

i) $$Pr(-\infty < \phi < \infty) = \int_{-\infty}^{\infty} f_\phi(u)\, du = 1$$

$$A \int_{-\phi_m}^{\phi_m} e^{-u^2/B^2} du + 2p = \sqrt{\pi}\, AB\, \text{erf}\,(\phi_m/B) + 2p = 1$$

$$p = \frac{1}{2}\left(1 - \sqrt{\pi}\, AB\, \text{erf}\,(\phi_m/B)\right) \qquad \text{(C-16)}$$

when $\phi_m \to \infty$ (linear system) we must have p = 0. This leads to:

$$A = \frac{1}{B\sqrt{\pi}} \qquad \text{(C-17)}$$

ii) $$E(\phi^2) = \sigma_\phi^2 = 2p\, \phi_m^2 + A \int_{-\phi_m}^{\phi_m} u^2\, e^{-u^2/B^2} du$$

and substituting A from Eq. C-17:

$$\frac{\sigma_\phi^2}{\phi_m^2} = 1 - \text{erf}\,(\phi_m/B) - \frac{B}{\phi_m}\,\frac{1}{\sqrt{\pi}}\, e^{-\phi_m^2/B^2} + \frac{1}{2}\left(\frac{B}{\phi_m}\right)^2 \text{erf}(\phi_m/B) \qquad \text{(C-18)}$$

$$p = \frac{1}{2}\left(1 - \text{erf}\,(\phi_m/B)\right) \qquad \text{(C-19)}$$

From Eqs. C-18 and C-19 the parameter B can be eliminated and p expressed in function of σ_ϕ and ϕ_m. Due to the complexity of the equations the system was solved numerically. The result is shown in Fig. 10.

The procedure is then: having the variances σ_y^2, σ_v^2 and σ_d^2 at time t, the variance of ϕ is computed from C-8, the probability p is obtained from Fig. 10, the linearization coefficients λ_v and λ_ϕ are computed from Eqs. C-15 and substituted into Eq. 18 to compute the derivative at time t. This derivative is used then to compute the response at time $t + \frac{1}{2}\Delta t$ or $t + \Delta t$ as was described in Appendix A.

APPENDIX D - PROPORTIONAL DAMPING

The procedure described for MDOF systems works for any combination of values for the damping factors. But in order to be able to compare the results with those of the random vibration in the frequency domain, the damping factors have to be taken in such a way that the modal equations are decoupled.

Let's consider the dynamic equations of a MDOF system:

$$M \ddot{\underline{x}} + C \dot{\underline{x}} + K \underline{x} = \underline{F} \qquad \text{(D-1)}$$

By solving the eigenvalue problem of the system,

$$K \Phi = \omega^2 M \Phi \qquad \text{(D-2)}$$

We obtain the eigenvalues $\omega_1^2, \omega_2^2, \ldots \omega_n^2$ and the eigenvectors

$$\Phi = (\underline{\phi}_1, \underline{\phi}_2, \ldots \underline{\phi}_n)$$

If we substitute $\Phi \underline{z} = \underline{x}$ and premultiply Eq. D-1 by Φ^T, we have:

$$\Phi^T M \Phi \ddot{\underline{z}} + \Phi^T C \Phi \dot{\underline{z}} + \underline{\Phi}^T K \Phi = \Phi^T \underline{F} \qquad \text{(D-3)}$$

Due to the orthonormality condition of Φ with M and K, the matrices

$$M = \Phi^T M \Phi$$
$$K = \Phi^T K \Phi$$

are diagonal and for Eq. D-3 to be decoupled all we have to have is that

$$C = \Phi^T C \Phi$$

is also a diagonal matrix. In general this will not be the case, but imposing some conditions on C this will be possible. The easiest condition is that C is proportional to K:

if $C = \alpha K$, then $\Phi^T C \Phi = \alpha \Phi^T K \Phi = \alpha K$ (diagonal).

We can choose the proportionality factor α in such a way that the first modal damping ratio has a specified value. If β_1 is the 1st modal damping ratio and ω_1 the 1st modal frequency, then α is given by:

$$\alpha = \frac{2\beta_1}{\omega_1} \qquad \text{(D-4)}$$

By taking two or more terms of the Caughey series:

$$C = M \sum_{i=0}^{p-1} a_i \left[M^{-1} K\right]^i ,$$

p modal damping ratios can be matched.

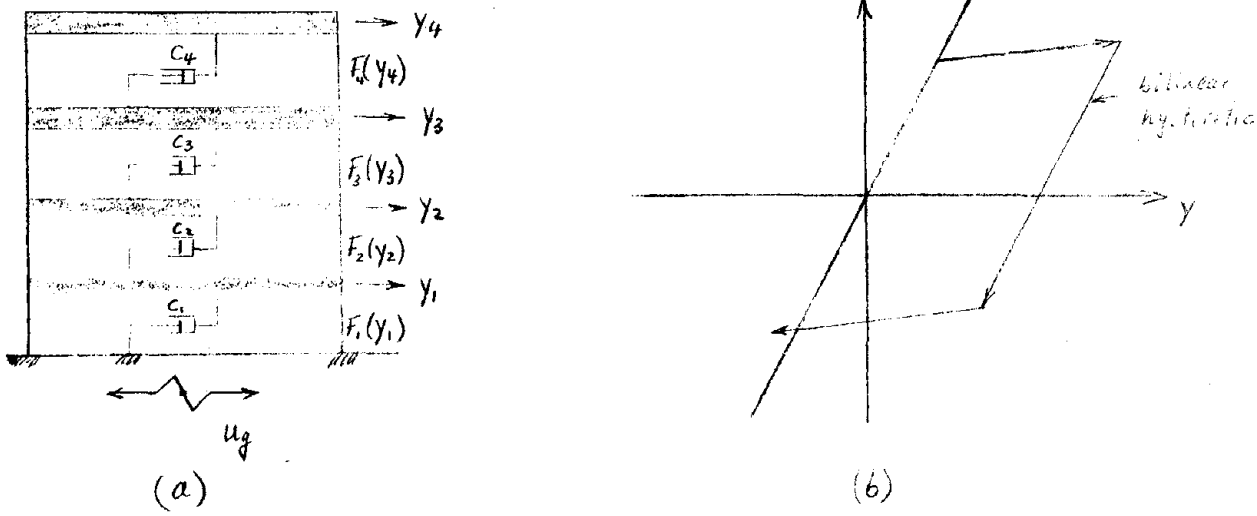

FIG. 1 Shear beam model and restoring force

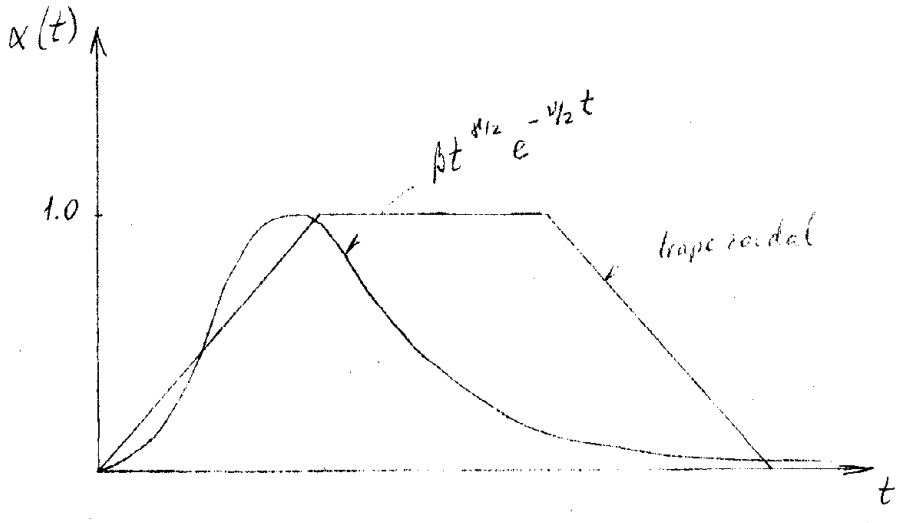

FIG 2 Intensity functions

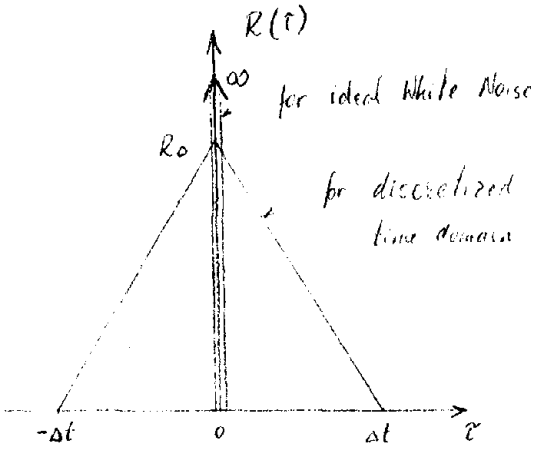

a.) autocorrelation function

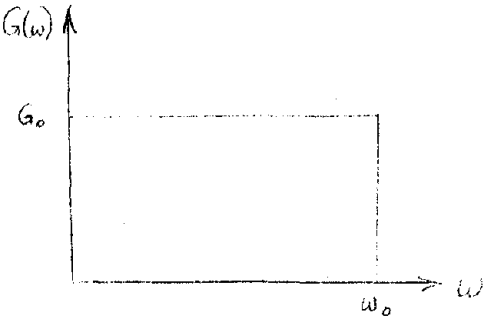

c.) rectangular psd function

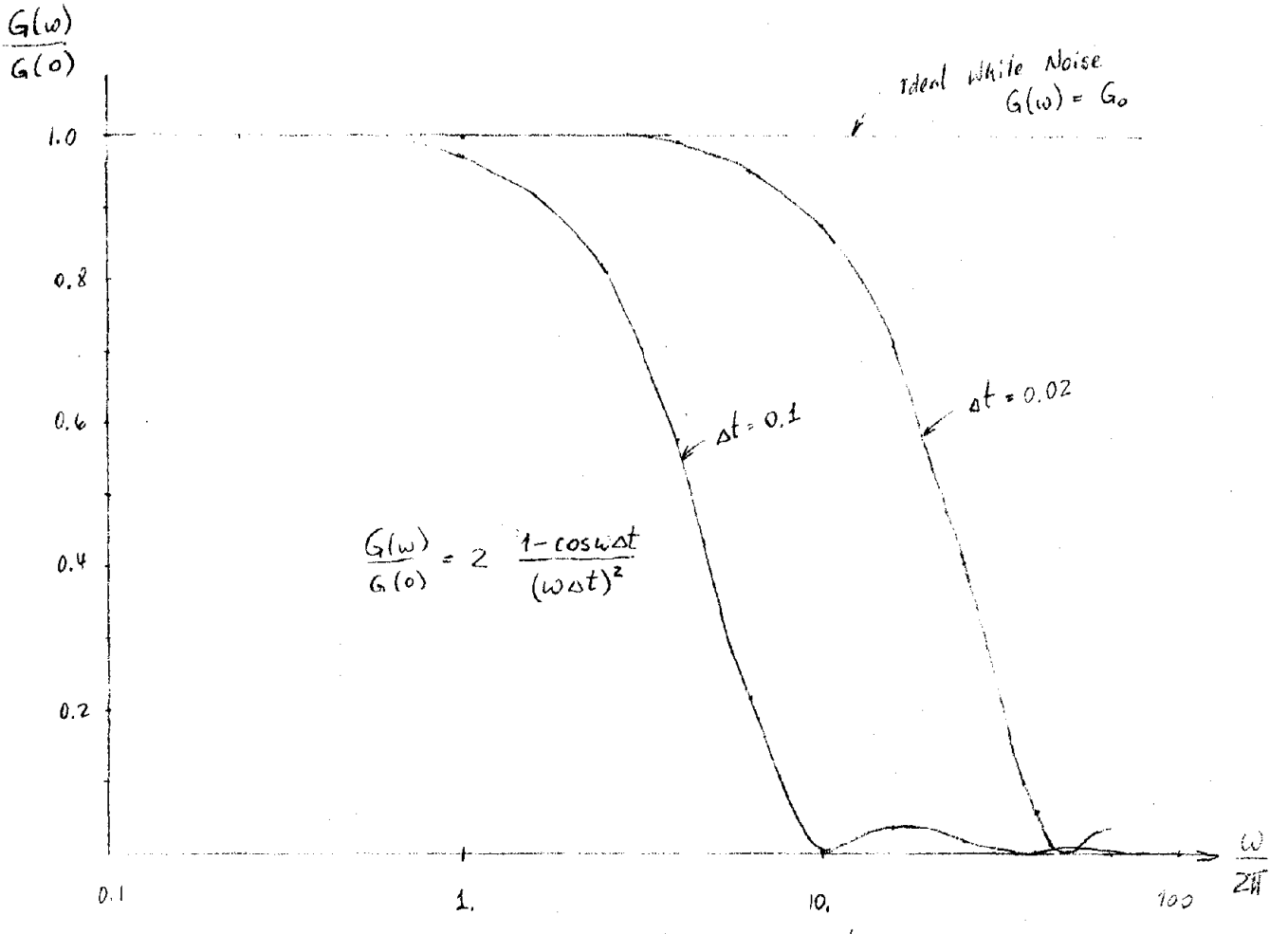

b) pseudo spectral density function

FIG 3 Effect of the time discretization

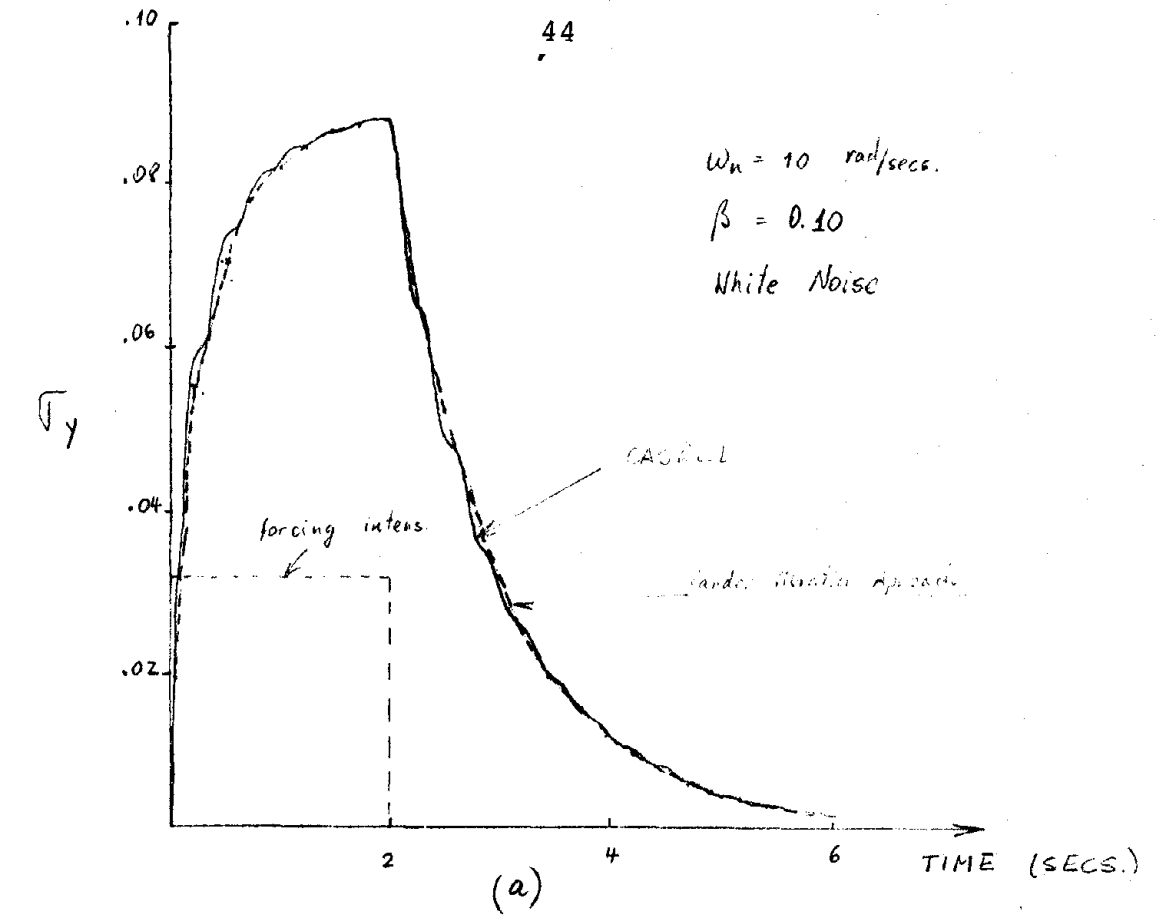

(a)

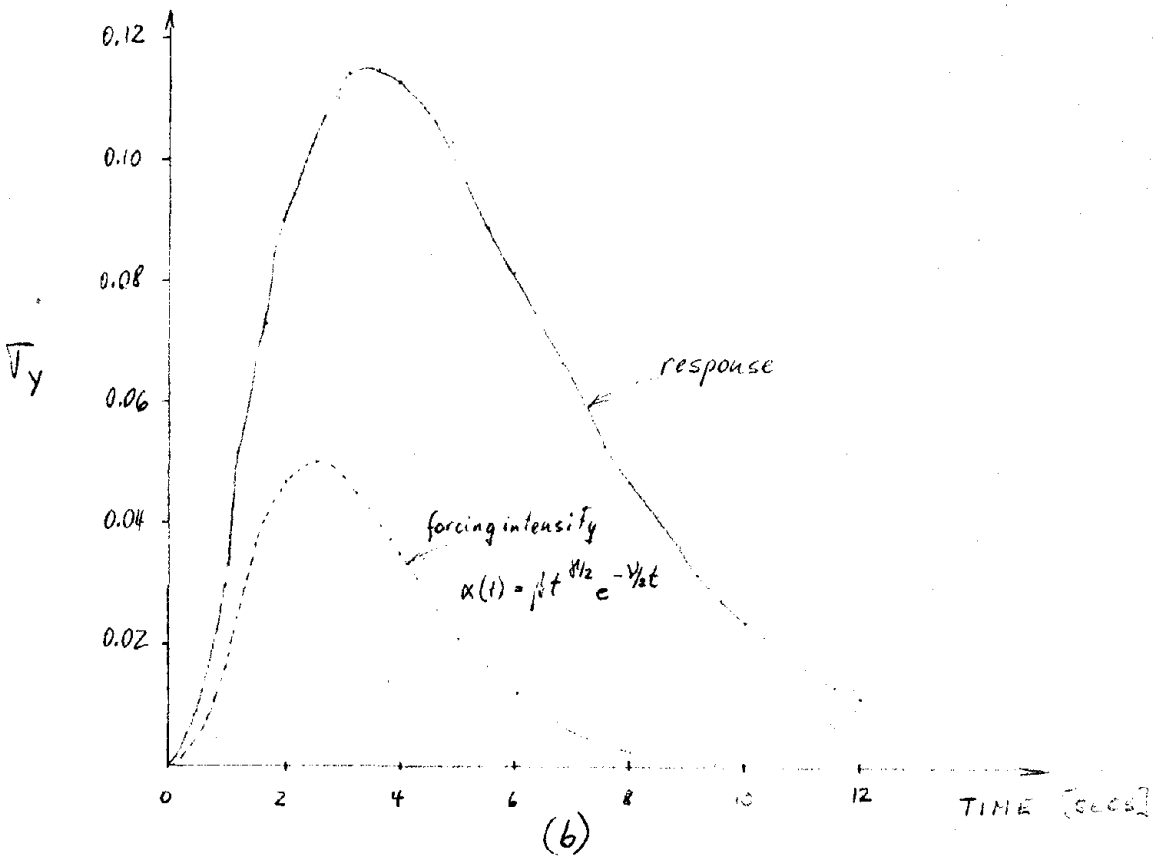

(b)

FIG 4: RESPONSE TO DIFFERENT INTENSITY FUNCTIONS

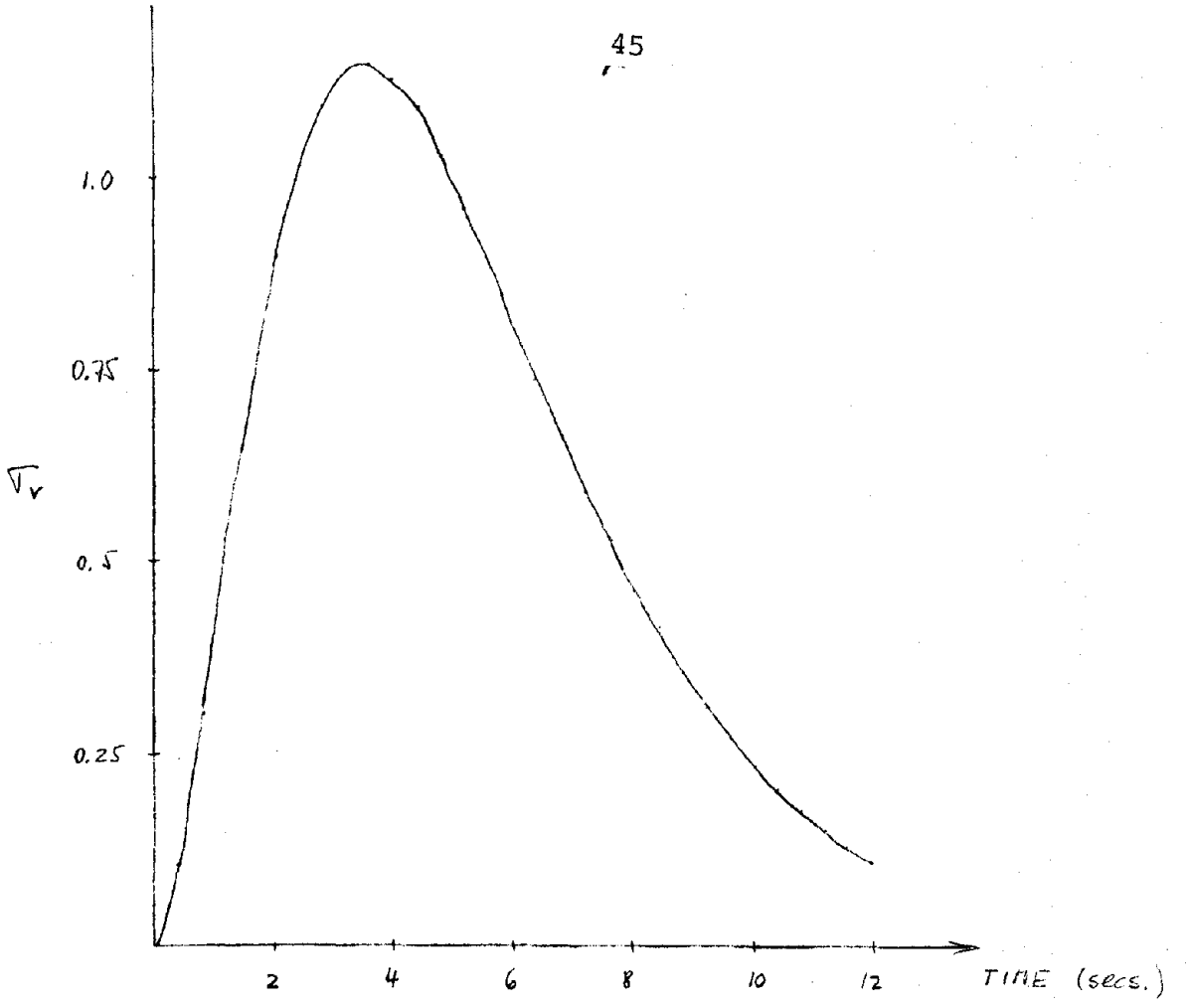

a) velocity

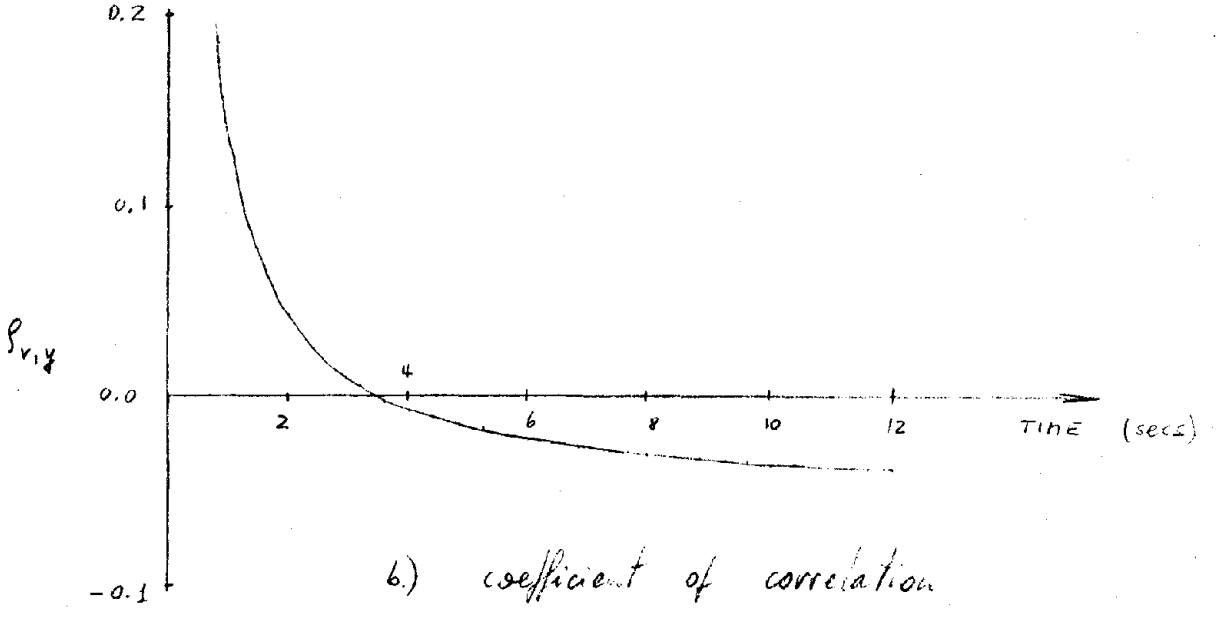

b.) coefficient of correlation

FIG 5. Velocity and Coefficient of Correlation Responses

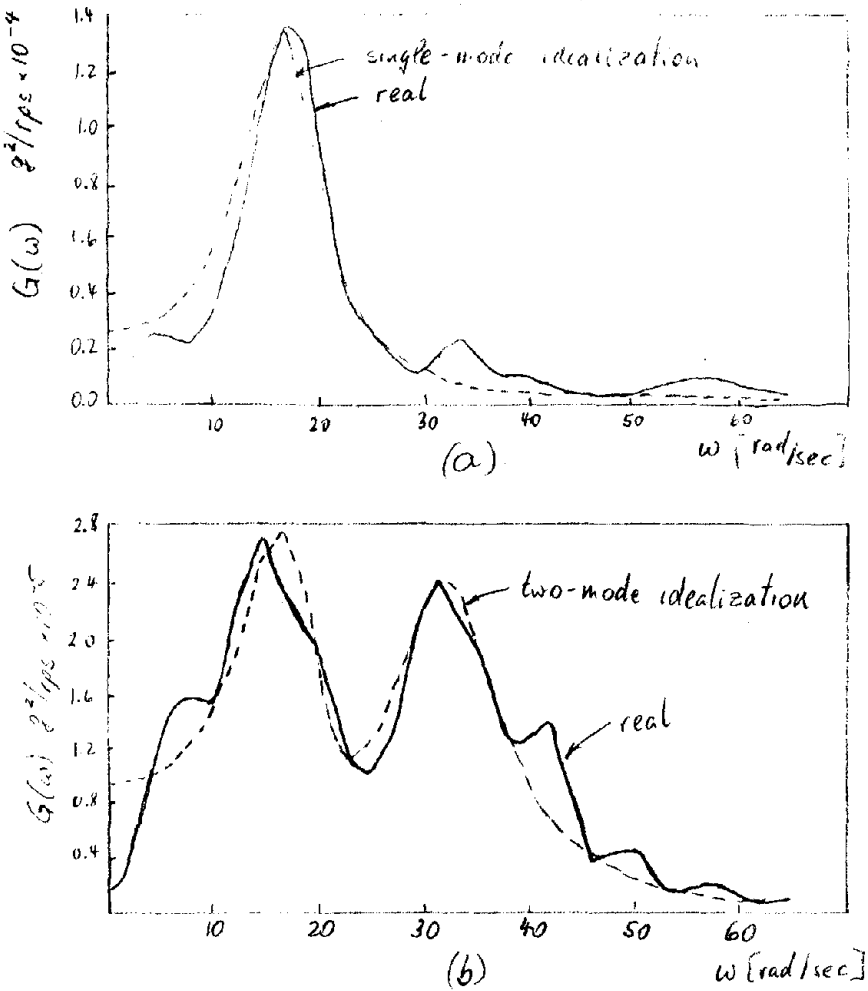

$\omega_{g1} = 18$
$\omega_{g2} = 32.4$
$\zeta_{g1} = 0.20$
$\zeta_{g2} = 0.20$

FIG 6 Two psd functions of the Parkfield Earthquake 1966 (from Ref. 14)

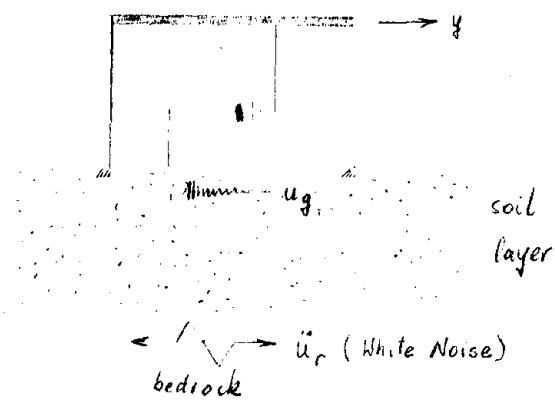

FIG 7 Structure subjected to filtered ground motion

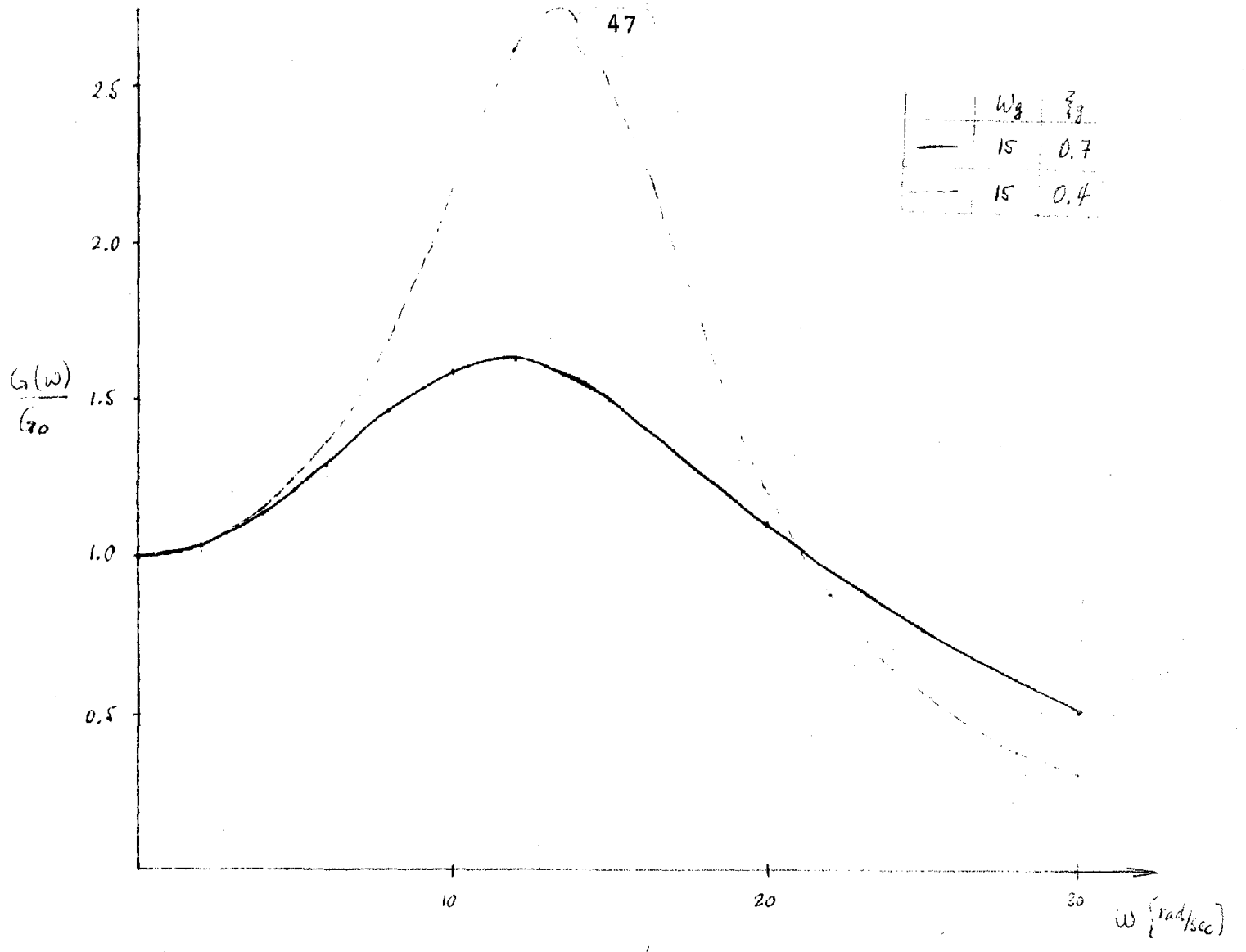

FIG. 8 Kanai - Tajimi spectrums

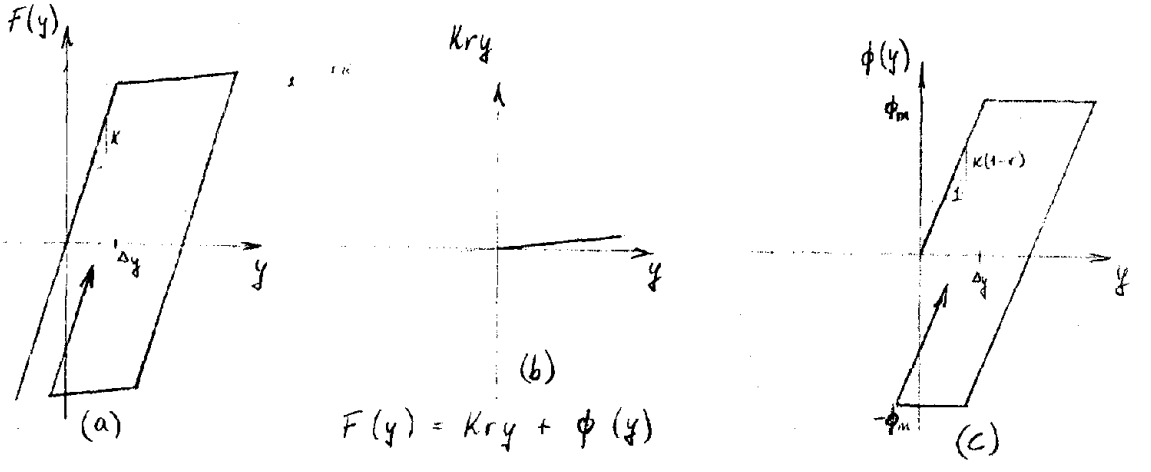

FIG 9 Decomposition of the bilinear hysteresis

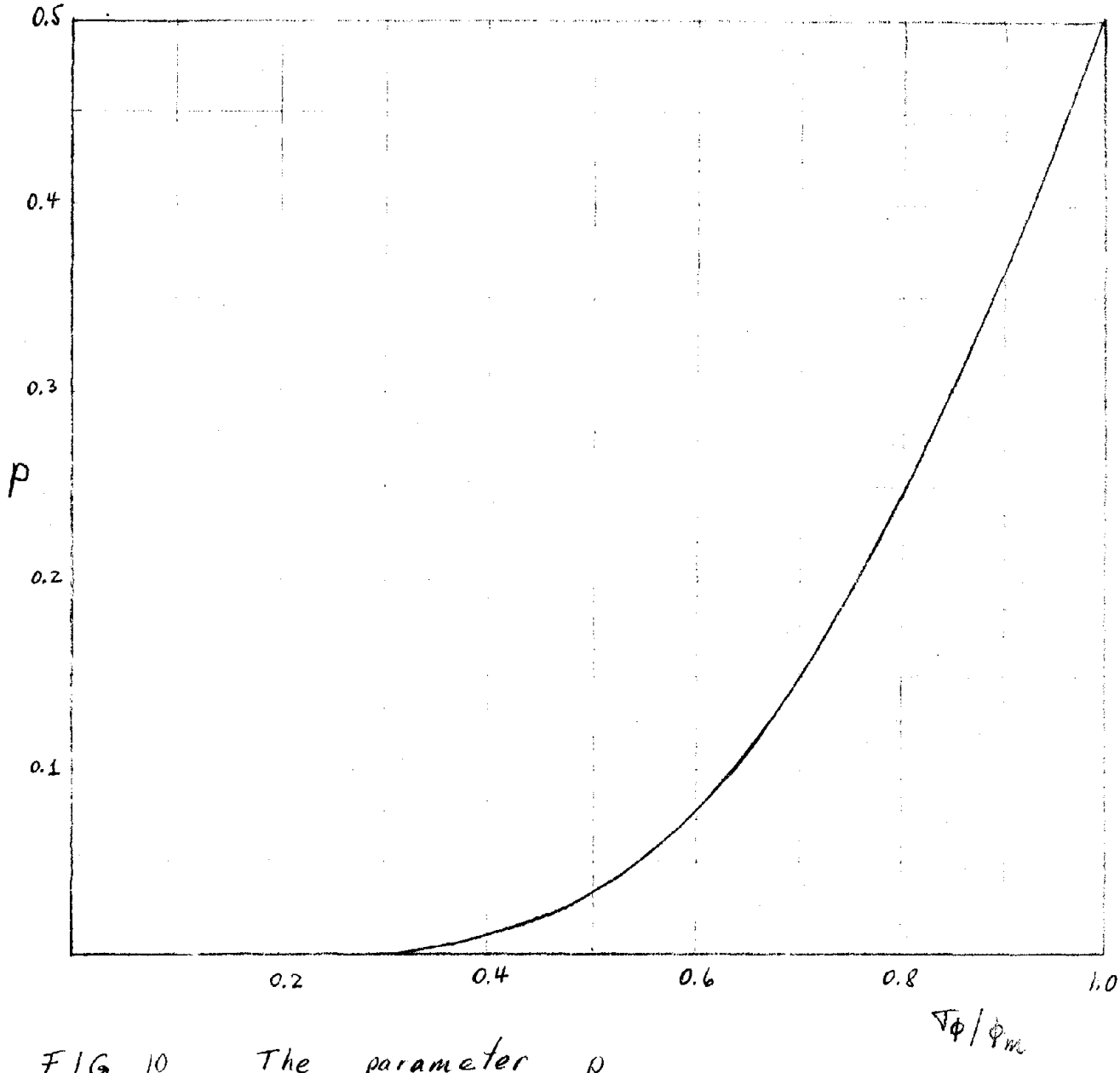

FIG 10 The parameter p

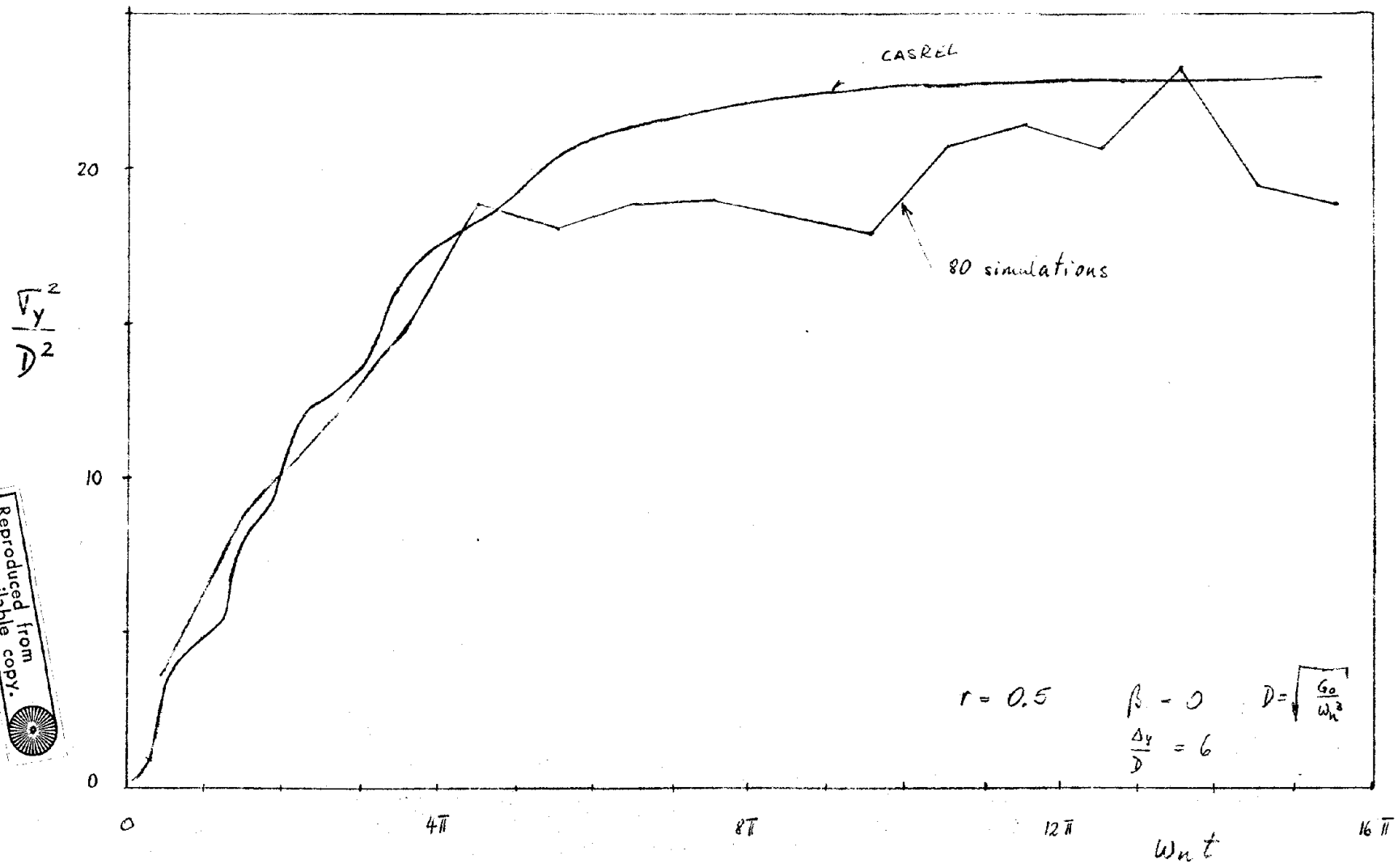

FIG 4: RESPONSE TO WHITE STATIONARY GROUND MOTION (Ref. 18)

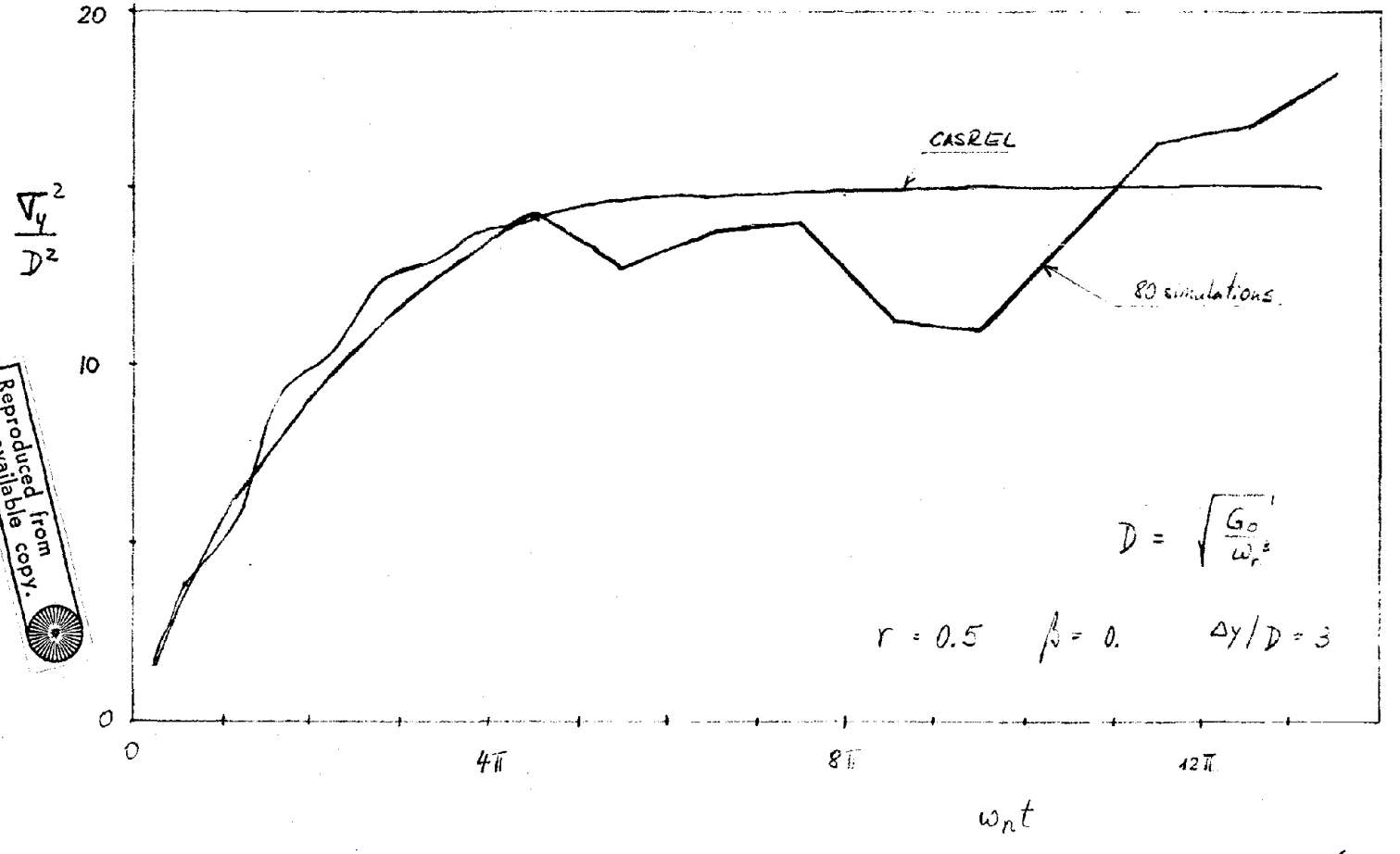

FIG 12 RESPONSE TO STATIONARY WHITE GROUND MOTION (Ref 18)

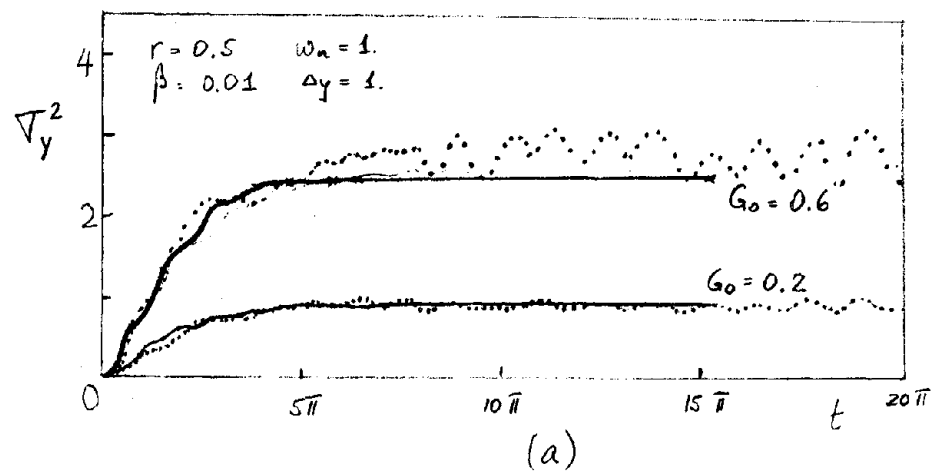

(a)

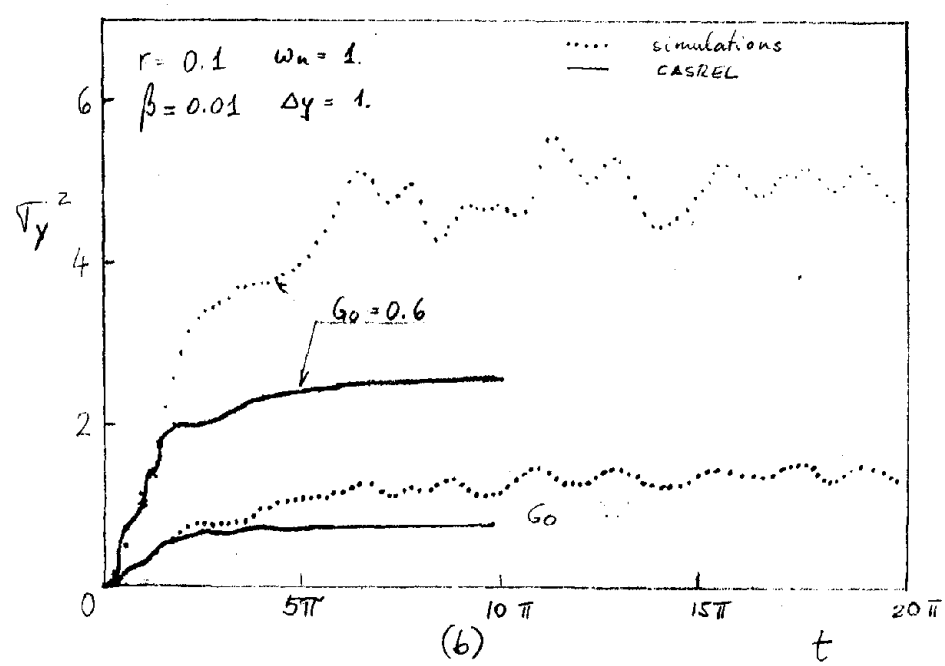

(b)

FIG 13 EFFECT OF THE RIGIDITY RATIO ON THE RESPONSE TO WHITE STATIONARY GROUND MOTION [Ref 13]

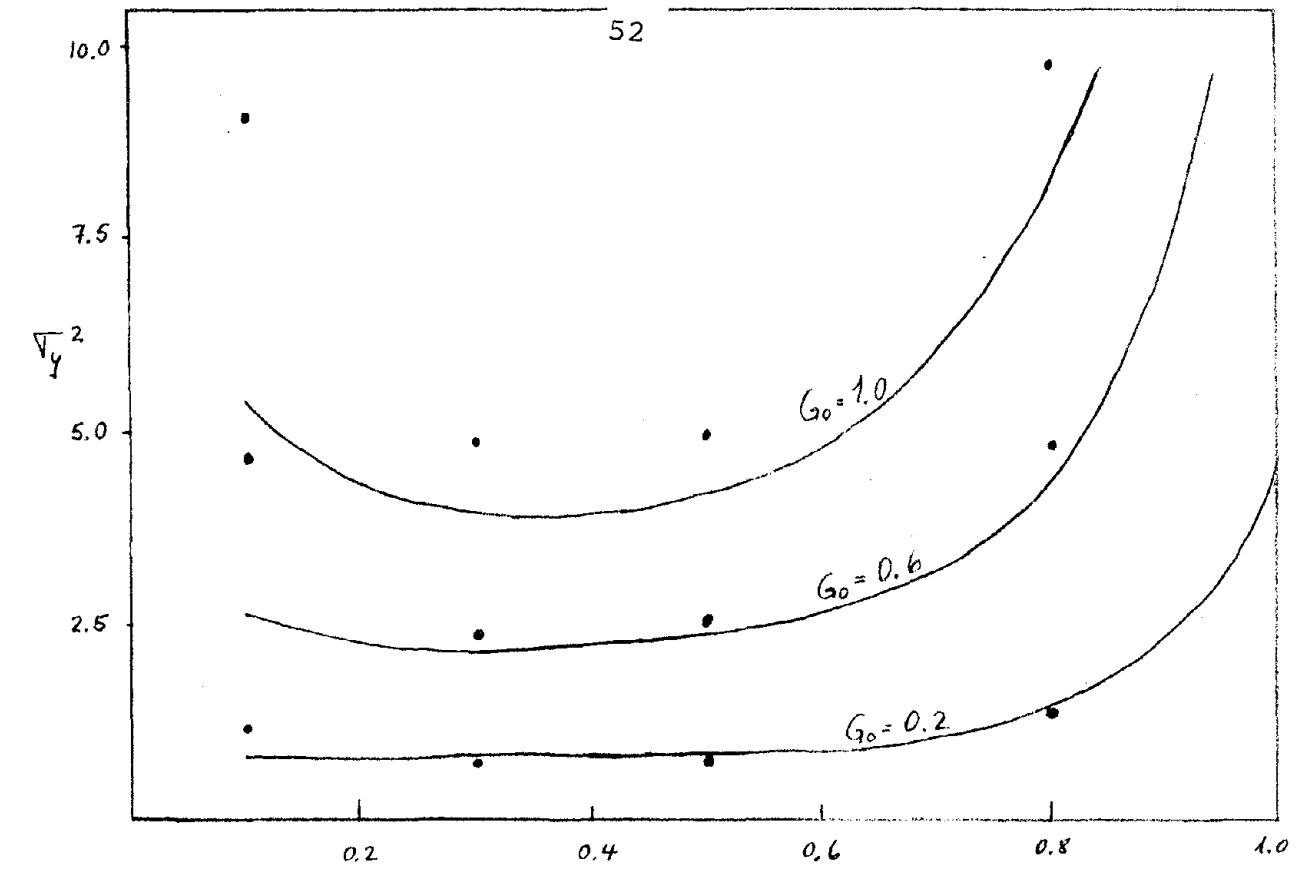

a.) relative displacement

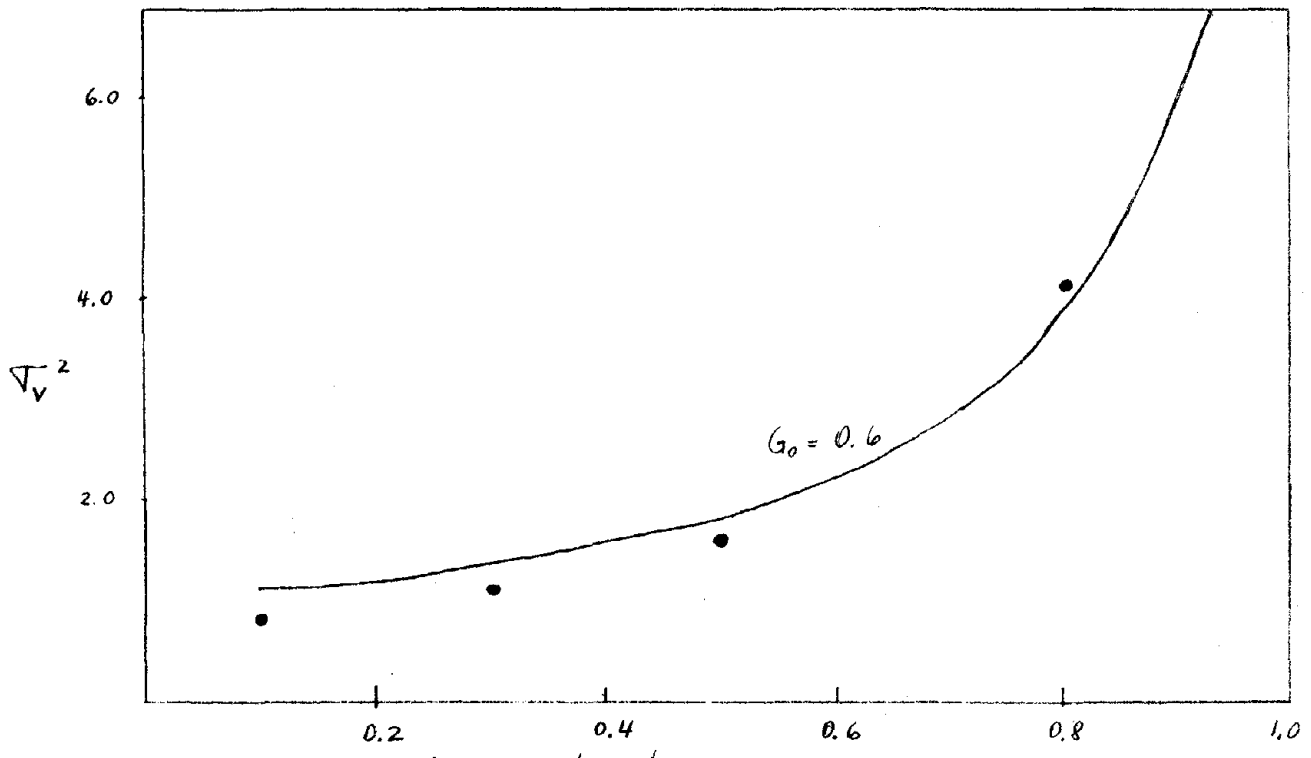

b.) velocity

FIG 14 EFFECT OF THE RIGIDITY RATIO ON THE RESPONSE [Ref. 13]

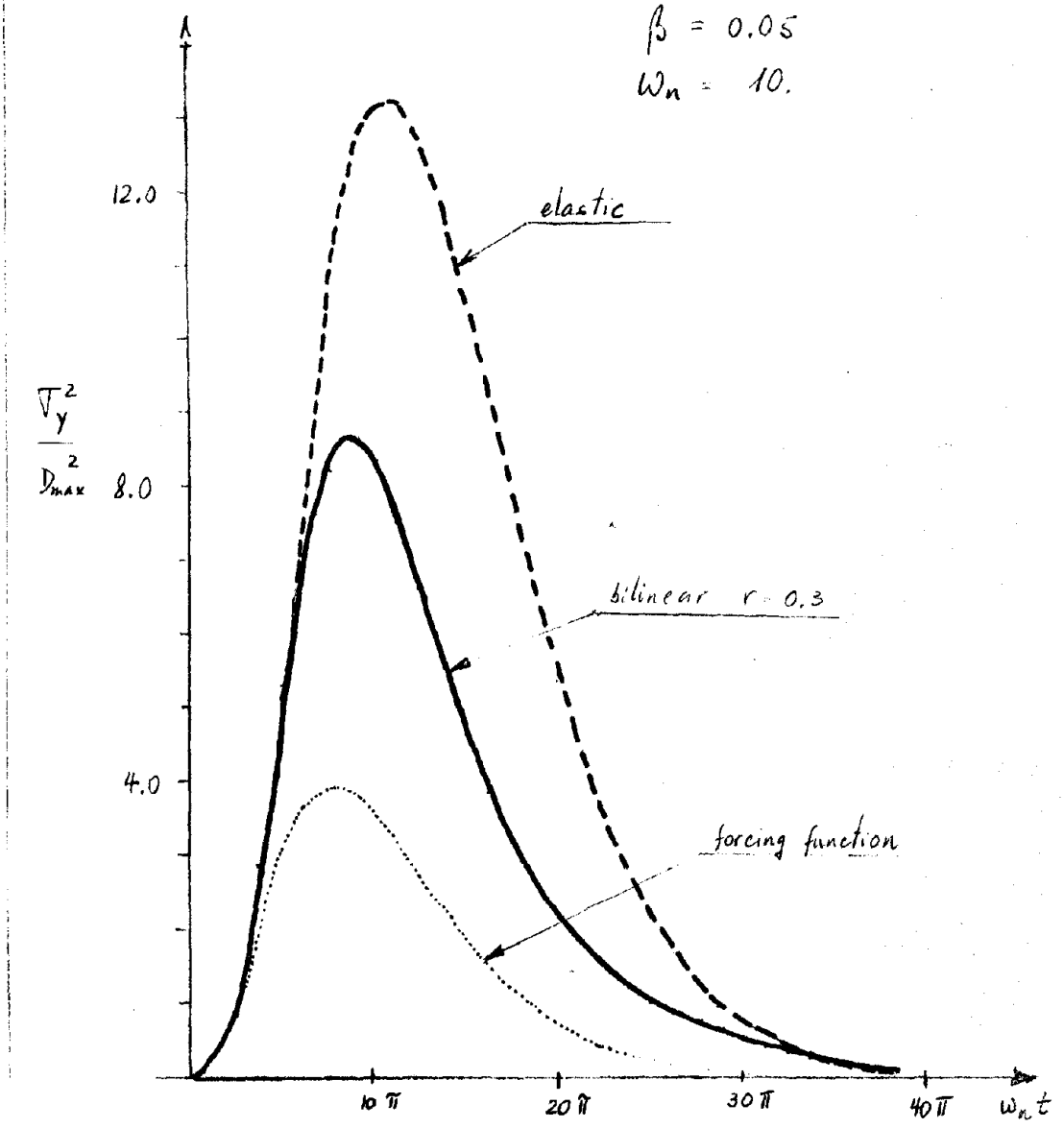

FIG 15 RESPONSE TO NONSTATIONARY WHITE GROUND MOTION

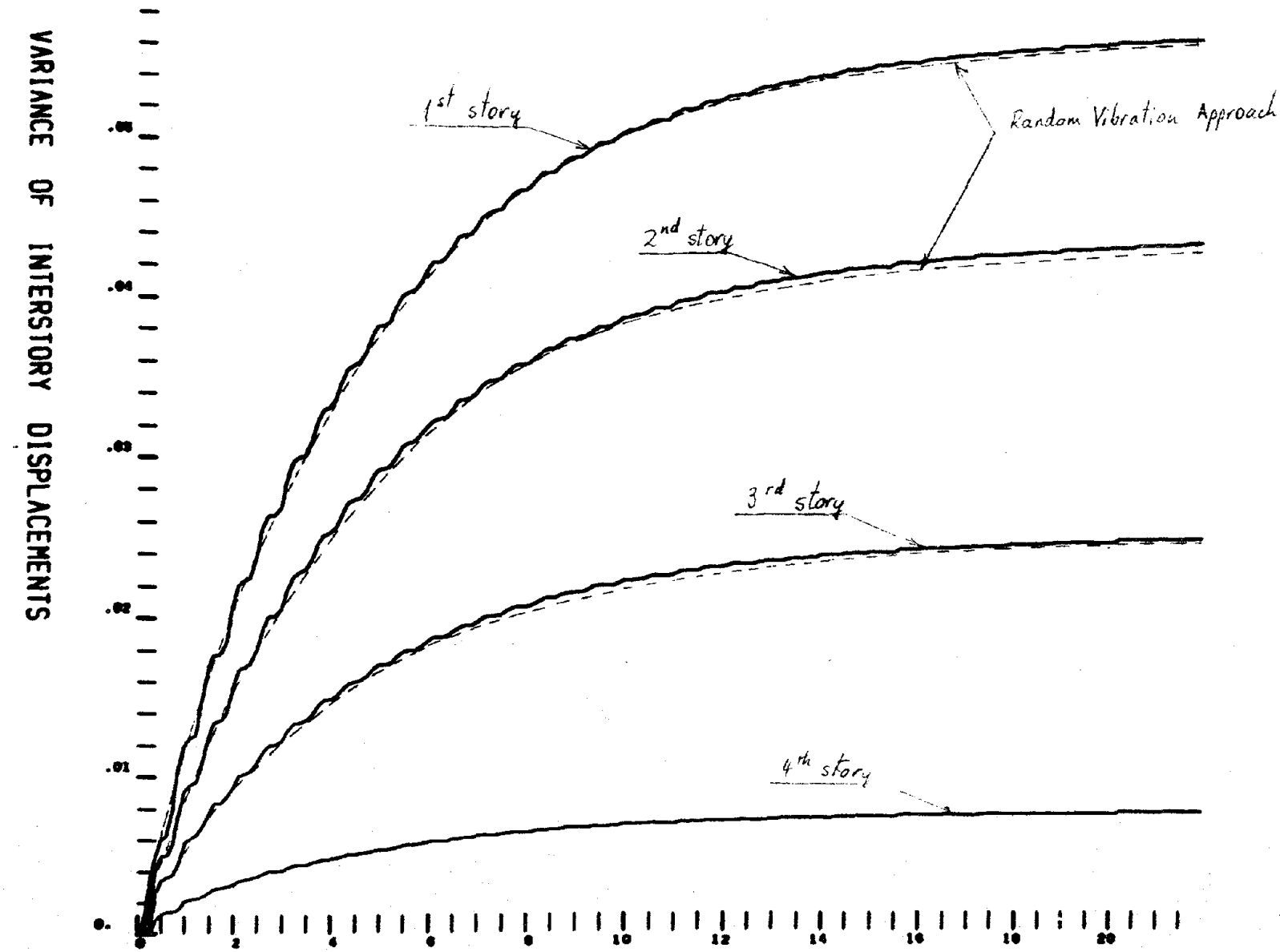

FIG 15 RESPONSE OF A 4 DOF SYSTEM TO STATIONARY FILTERED GROUND MOTION

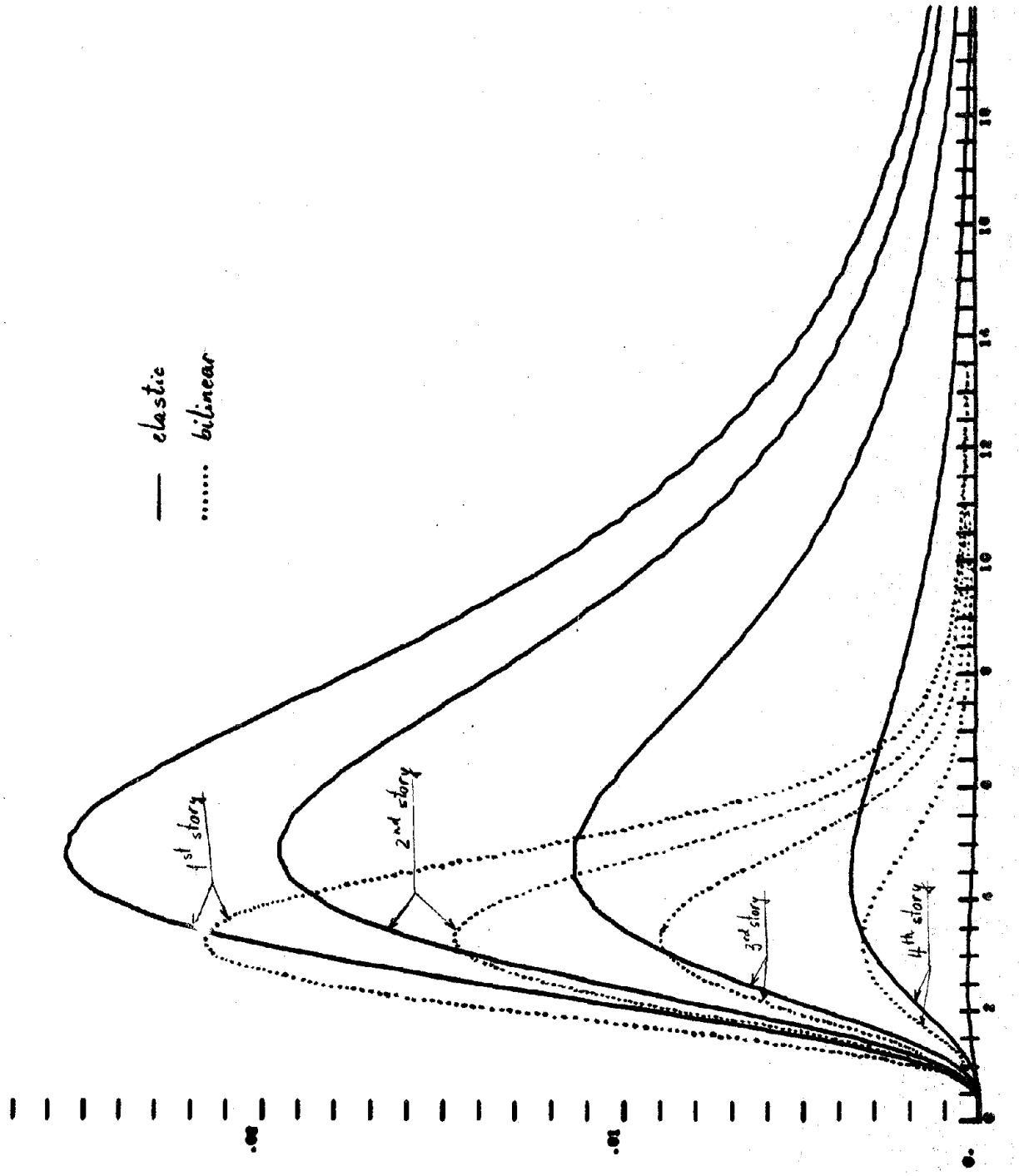

FIG 17 RESPONSE OF A 4 DOF SYSTEM TO NONSTATIONARY FILTERED GROUND MOTION

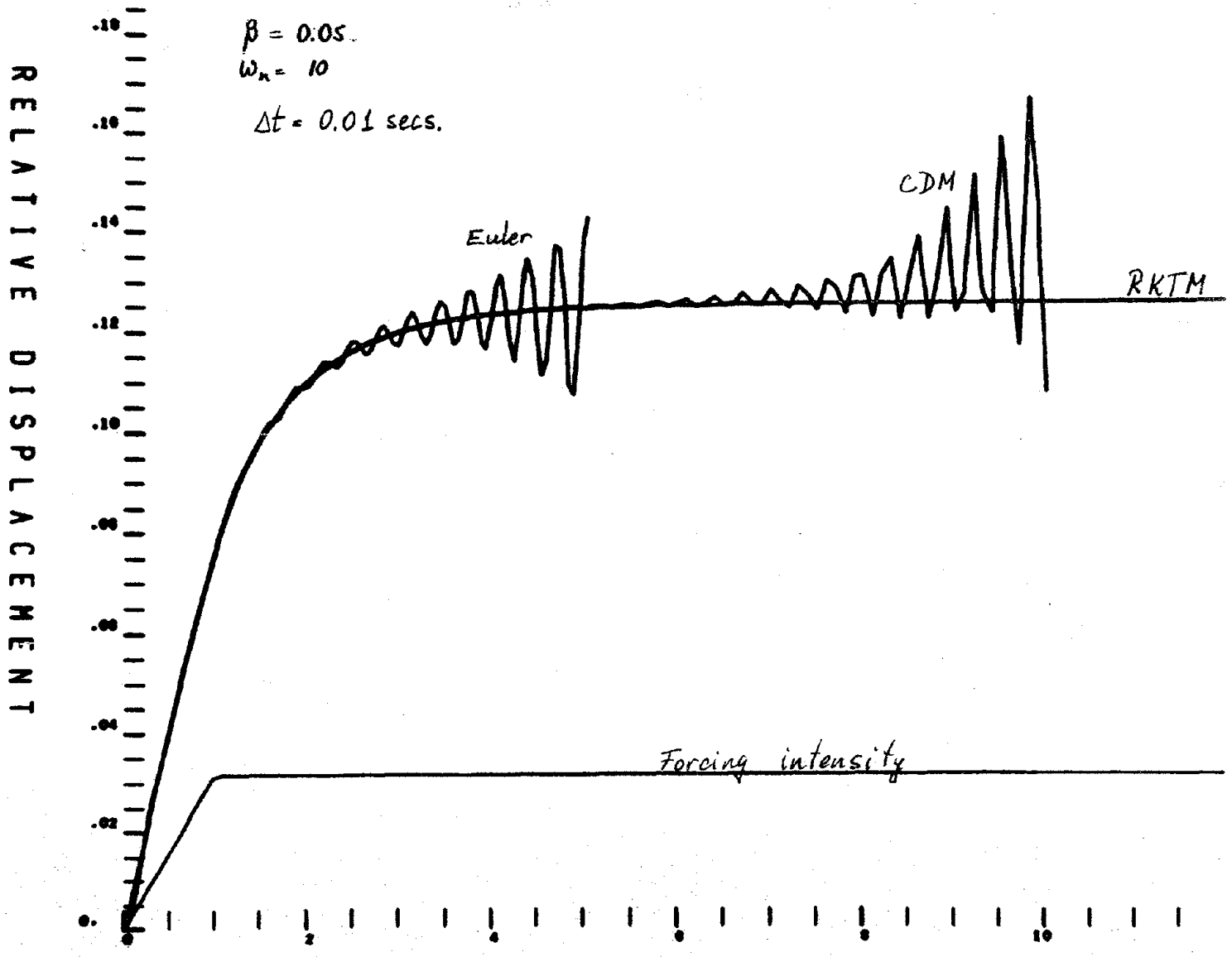

FIG A-1 COMPARISON OF DIFFERENT INTEGRATION METHODS $\Delta t = 0.01$ secs.

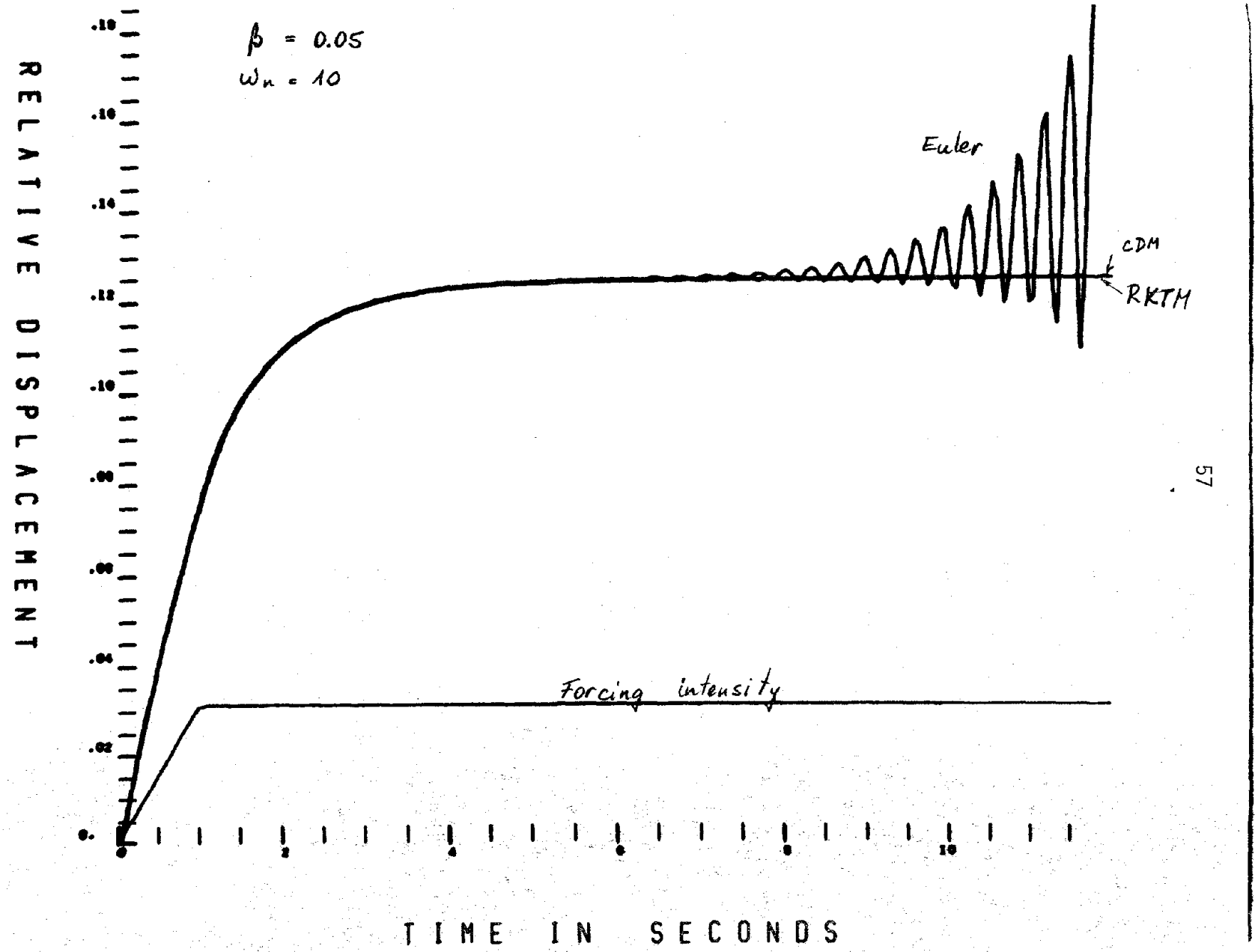

FIG A-2 COMPARISON OF DIFFERENT INTEGRATION METHODS $\Delta t = 0.005$ secs.

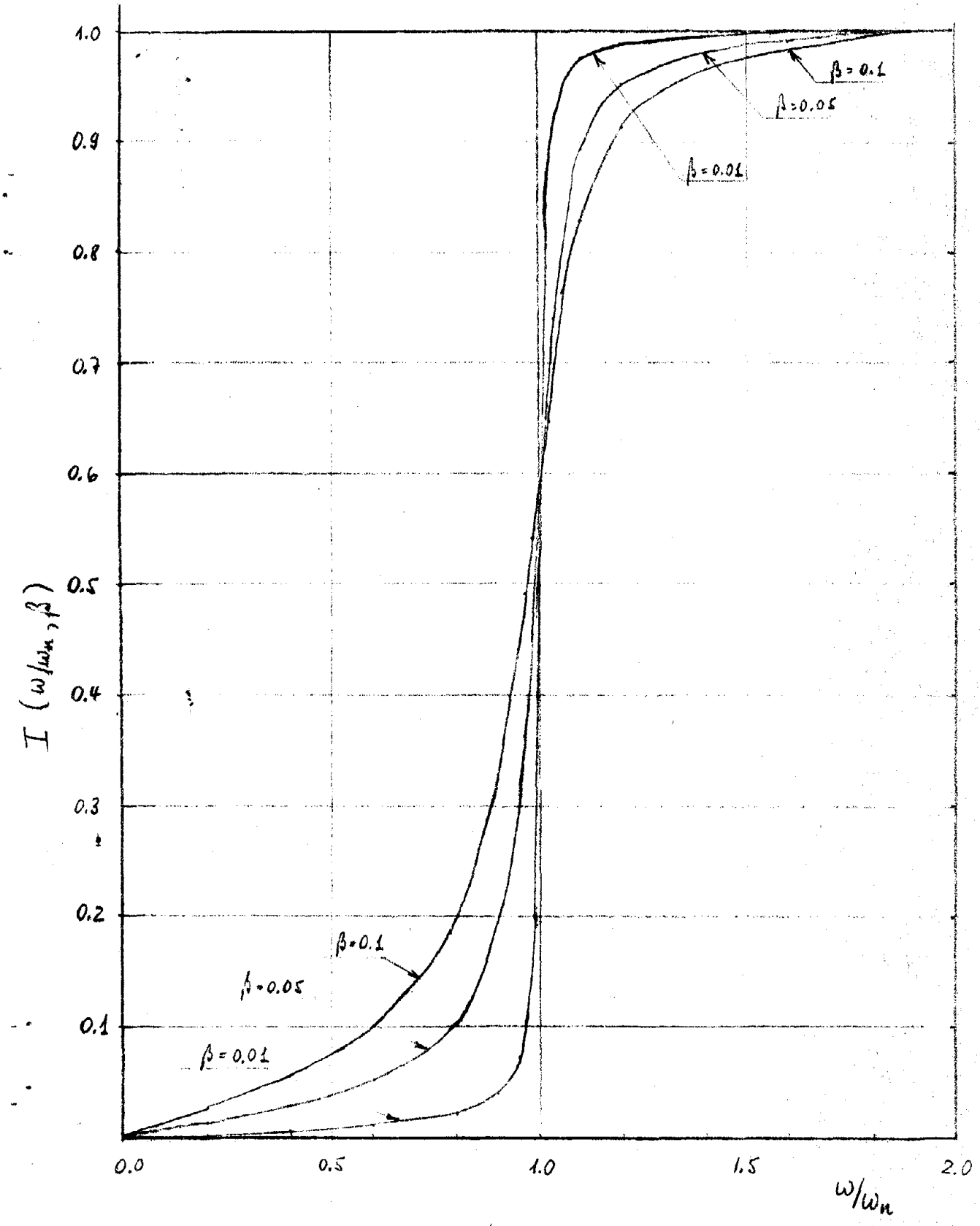

FIG B-2 Parameter $I(\omega/\omega_n, \beta)$ of Eq. B-2

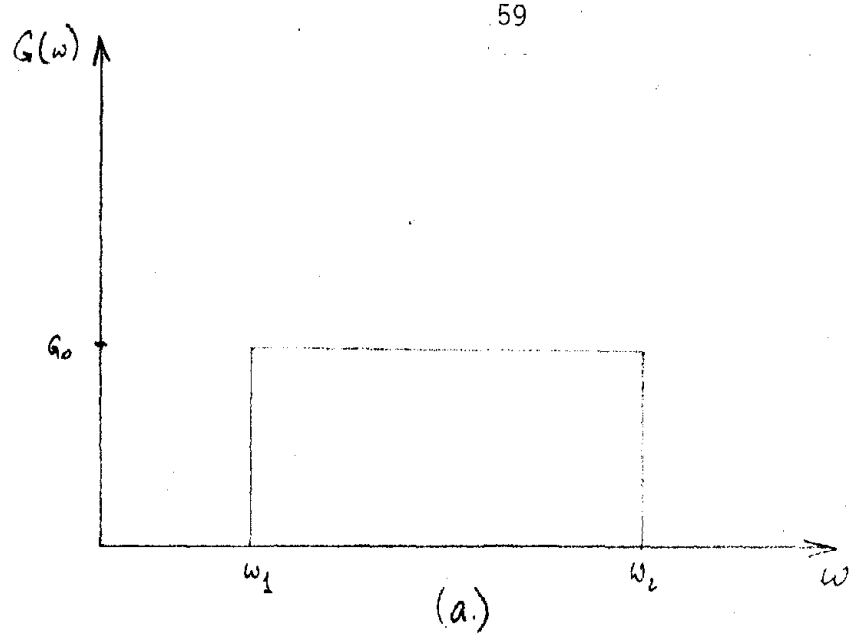

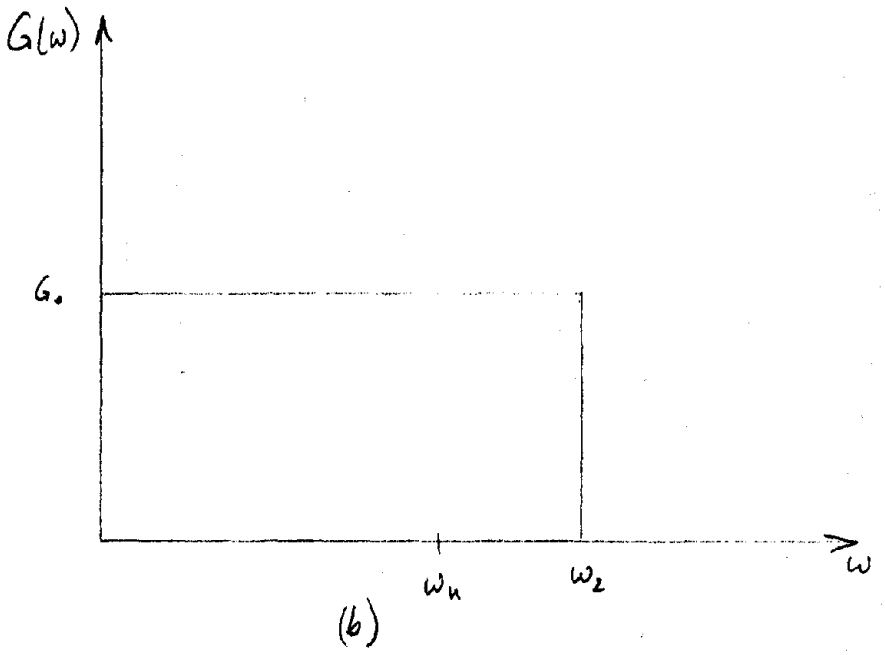

FIG B-1 Pseudo Spectral Density Functions

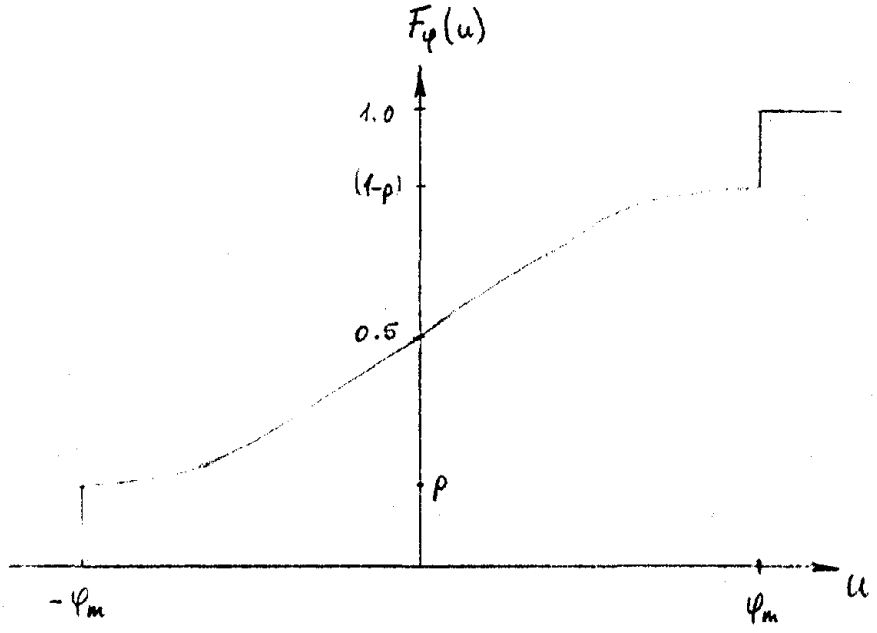

$$Pr[u < \varphi < u + du] = \begin{cases} p & u = -\varphi_m \\ A e^{-\frac{u^2}{B^2}} du & -\varphi_m < u < \varphi_m \\ p & u = \varphi_m \\ 0 & |u| > \varphi_m \end{cases}$$

FIG C-1 The probability law of φ